Received: 23 August 2019 | Revised: 13 November 2019 | Accepted: 17 November 2019

DOI: 10.1111/jace.16934

INVITED FEATURE ARTICLE

Journal of the American Ceramic Society

Closed porosity ceramics and glasses

Cekdar Vakifahmetoglu[1] | **Tugce Semerci**[1] | **Gian Domenico Soraru**[2]

[1]Department of Materials Science and Engineering, Izmir Institute of Technology, Urla, Izmir, Turkey

[2]Department of Industrial Engineering, University of Trento, Trento, Italy

Correspondence
Cekdar Vakifahmetoglu, Department of Materials Science and Engineering, Izmir Institute of Technology, 35430, Urla, Izmir, Turkey.
Email: cekdarvakifahmetoglu@iyte.edu.tr; cvahmetoglu@gmail.com

Funding information
Izmir Institute of Technology

Abstract

In the last three decades, considerable effort has been devoted to obtain both open and closed porosity ceramics & glasses in order to benefit from unique combination of properties such as mechanical strength, thermal and chemical stability at low-relative density. Most of these investigations were directed to the production and the analysis of the properties for open porosity materials, and regrettably quite a few compositions and manufacturing methods were documented for closed porosity ceramics & glasses in the scientific literature so far. This review focuses on the processing strategies, the properties and the applications of closed porosity ceramics & glasses with total porosity higher than 25%. The ones below such level are intentionally left out and the paper is set out to demonstrate the porous components with deliberately generated closed pores/cells. The processing strategies are categorized into five different groups, namely sacrificial templating, high-temperature bonding of hollow structures, casting, direct foaming, and emulsions. The principles underlying these methods are given, with particular emphasis on the critical issues that affect the pore characteristics, mechanical, thermal and electrical properties of the produced components.

KEYWORDS

cellular, closed porosity, foam, porous ceramics, porous glasses

1 | INTRODUCTION

Porous materials, especially ceramics & glasses (C&G hereafter) have been of great interest in wide range of technological processes such as biomedical, catalysis, insulation, filtration (gases & liquids including molten metals), etc[1,2] These brittle solids can be categorized in a number of different ways, for example, well-defined periodic, cellular, or random structured. Another classification is based on the pore size; the International Union of Pure and Applied Chemistry (IUPAC) definition, that is materials having pore size below 2 nm are defined as microporous, the ones in between 2 and 50 nm as mesoporous, and the ones having pores > 50 nm are called macroporous (note that the macroporous polymeric materials defined by the IUPAC is the one having pore size in between 50 nm and 1 μm).[3] A material constituted by pores of at least two of these length scales is referred as having hierarchical porosity, and hierarchical porosity may exist as trimodal (micro&meso&macro) or only bimodal (micro&meso, micro&macro, meso&macro).

Abbreviations: AC, aerated concrete; ACM, acrylamide; AlON, aluminum oxynitride; AM, additive manufacturing; BN, boron nitride; BST, barium strontium titanate; C&G, ceramics & glasses; CBAs, chemical blowing agents; CFA, coal fly ash; CMC, ceramic matrix composite; CRT, cathode ray tube; DIW, direct ink writing; FAC, fly ash cenosphere; FC, foamed concrete; GA, Gibson and Ashby; Gr, Grashof number; HIP, hot isostatic pressing; LZMT, lead-zinc mine tailing; MBAM, *N*,*N*′-methylenebisacrylamide; MSA, minimum solid area; NMAM, *N*-hydroxymethyl acrylamide amide; PBAs, physical blowing agents; PDCs, polymer-derived ceramics; PMMA, polymethyl methacrylate; PPI, pores per inch; PPs, preceramic polymers; RT, room temperature; R_{TS}, thermal shock resistance; SDS, sodium dodecyl sulfate; SLS, selective laser sintering; TPS, thermal protection system; UHTC, ultra-high temperature ceramics; IUPAC, International Union of Pure and Applied Chemistry; YSZ, yttria-stabilized zirconia; ZrC, zirconium carbide; ZTA, zirconia toughened alumina; ϕ_C, closed porosity; ϕ_T, total porosity.

Since above designation is actually done for the materials in catalysis, and the macroporosity range is open-ended, in order to distinguish micron to mm sized pores a variant "cell"-based definition is adapted from the plastic industry. In this classification, materials with pores, approximately, in between 1 and 100 μm are called microcellular, and the ones having larger than 100 μm are termed as macrocellular. An alternative arrangement can also be done by counting the number of cells/pores per inch (2.54 cm), that is pores per inch (PPI) designation.

Pore topology is also used for classification, such as materials with open (permeable, interconnected), blind (dead-end), closed (isolated or only connected with neighboring cells but having no permeability), and mixed porosity. The pores can sometimes be structured in a leveled (graded porosity) or aligned manner (lotus type, lamellar, directionally oriented porosity).[4]

Comprehensive reviews[1,5–10] and books[11,12] were published about the fabrication methods (templating-sacrificial/fugitive, partial sintering, etching, additive manufacturing, foaming, supercritical drying, etc), properties and applications of especially porous ceramics. The majority of the studies investigated in such extensive works were performed for the production of permeable, open porosity ceramics whereas only limited attempts have been devoted to the processing and properties of the C&G having closed porosity.

One of the earliest applications of closed porosity C&Gs was probably in the refractory industry, where pores are used to master the thermal conductivity to improve the energy efficiency. While the initial publication records dates back to early 1980s, the number of both scientific papers and patents has been increasing at an exponential rate, evidencing the growing interest for these materials, see Figure 1A,B.

As can be seen from Figure 1, there are now several published works on the topic (note that the number of patents is higher), and highly porous products ranging from foams to 3D-printed components have been produced. However, currently there is no review paper on the closed porosity C&Gs. Therefore, in this review, we aim to highlight the importance of such materials and cover the number of techniques and compositions that can be used for the production of closed porosity C&Gs. It should be pointed out that the porous C&Gs for which the porosity level is lower than ~ 25 vol% (low porosity ceramics or sintering artifacts with unsought residual closed porosity) has been deliberately excluded for brevity.

2 | PROCESSING STRATEGIES

Porosity as defined by IUPAC can be simplified as the percentage found by dividing the total space volume (cell cavities) to the bulk volume. This can be identified as open (interconnected), closed (isolated or only connected with neighboring cells but eventually having no permeability), or mixed. The deliberate formation of the closed porosity is inherently more complicated since the pore-forming "agent" (eg, any decomposing/volatile gas or reaction by-products) generally stays transiently and while leaving the system, it creates interconnection. Accordingly, C&Gs with closed porosity have fewer production methods compared to that for the open porous ones.[13] The production methods, which will be discussed in detail later, are categorized into five groups, namely sacrificial templating, high-temperature bonding of hollow structures, casting, direct foaming, and emulsions. In each section, the given tables aim to demonstrate the current status of the published studies on closed porosity C&Gs. As one can see from

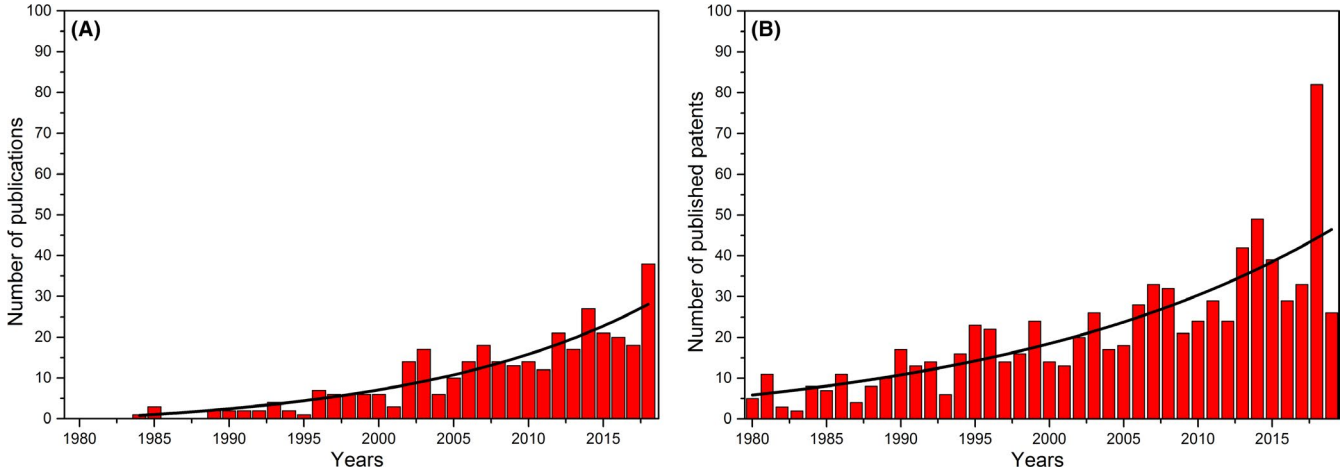

FIGURE 1 (A) Number of publications resulting from a *web of science* search with the keyword "closed porosity ceramic" and "closed porosity glass". (B) Number of published patents found from Questel database by searching the abstracts using following query (close + 1w por+) and (ceramic or glass). "1w" means given two keywords should be in close proximity. Both data were extracted from 1980 up to now and the line represents an exponential growth function fit

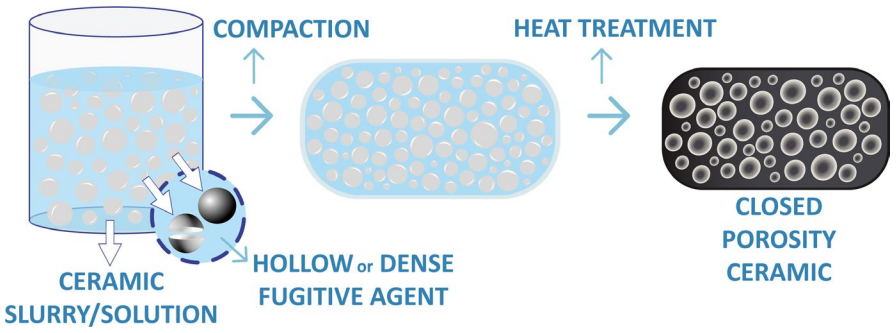

FIGURE 2 Schematic representation of the sacrificial (fugitive) templating method

the tables, there are several works for each technique but only a few of them will be mentioned in detail to avoid redundancy.

2.1 | Sacrificial templating

Dispersion of a sacrificial (fugitive) templating phase (salts and synthetic/natural organic particles/beads from nano to micron size) throughout a matrix, followed by curing/drying to obtain appropriate green-body strength and subsequent extraction/decomposition of the templating agent is a well-established technique to obtain a porosity.[5] If the usxed sacrificial phase quantity is adequate to form a contact network, a permeable component can be formed. This strategy has also been adapted to attain a closed porosity (Figure 2 demonstrates the schematic representation of the method and Table 1 gives some properties of the closed porosity ceramics produced by sacrificial templating). In order to prevent the formation of percolating pore-web, either hollow (limited decomposition by-product) or fewer quantity structures were used so that the interconnection in between the final pores is restricted.[14]

Series of samples were prepared by using preceramic (polysiloxane) polymer together with different (from 20 to 90 wt%) amount of expanded microspheres (hollow polymethyl methacrylate (PMMA)-based beads).[14–17] The closed porosity formed due to PMMA decomposition during pyrolysis was able to be extended up to 90% with < 30 μm cell size, and some of the samples was reported to have surprisingly high-compressive strength values reaching above 100 MPa (at ϕ_T ~ 70%). As a general rule, hollow templates are spherical resulting in the final pore structure similarly shaped. However, tailor-made microstructured ceramic foams can be formed if one could control the size/shape of the sacrificial agents. For this purpose, sacrificial ceramic hollow forms were produced initially by coating styrene granules, seeds, peas or nuts (any material with low-decomposition temperature is actually suitable for this purpose), succeeded by the core removal. Figure 3A demonstrates the monolithic foam made by using these sacrificial agents having various diameters resulting in a gradient porosity.[18] When limited amount of nonhollow sacrificial agents, such as paper processing residue was used with different clays, it was possible to obtain anorthite ceramics with closed porosities reaching up to 55%, see Figure 3B for the SEM image of the monolithic sample when 30 wt% paper was used as fugitive phase).[19,20]

The key feature of sacrificial templating technique is that depending on the fugitive agent amount/size/shape, it is possible to control the pore characteristics (size/shape/orientation) and form graded porosity components. However, the decomposition by-products of the sacrificial agents not only should be analyzed concerning the odor, reactivity, toxicity, flammability, etc but also should be carefully controlled in order not to cause any flaws in the final material.[21] Besides, due to the nature of the decomposition process, there may be uncontrollable residual impurities in the final material.

TABLE 1 Properties of the closed porosity ceramics produced by sacrificial templating

Formed ceramic or glass/pore-forming agent	Porosity	Pore size	Mechanical property	Other properties	Ref.
Alumina/hollow microspheres made from peas, seeds, polystyrene	ϕ_T = 77%-89%	< 2000 μm	σ_c = 0.9-4 MPa		18
Multiphase ceramic (anorthite, mullite, or gehlenite)/recycled paper	ϕ_T ~ 27%-55%		σ_c = 8.9-43.2 MPa	λ = 0.42-0.83 W/m.K.	19,20
Silicon oxycarbide/Hollow PMMA microspheres	ϕ_T = 27%-88%	<35 μm	σ_c ~ 100 MPa (@~70%ϕ_T)		14–17
Alumina & zirconia-toughened alumina (ZTA)/agar & polyethylene spheres	ϕ_T = 56%-83% (12%-43% ϕ_C)	130-190 μm	σ_c = 3.7-35.1 MPa (@60%-70% ϕ_T)		22

Note: ϕ_T = total porosity, ϕ_C = closed porosity, porosity calculations were done via Archimedes by using water or gas pycnometer & bulk density, σ_c = compressive strength, λ = thermal conductivity.

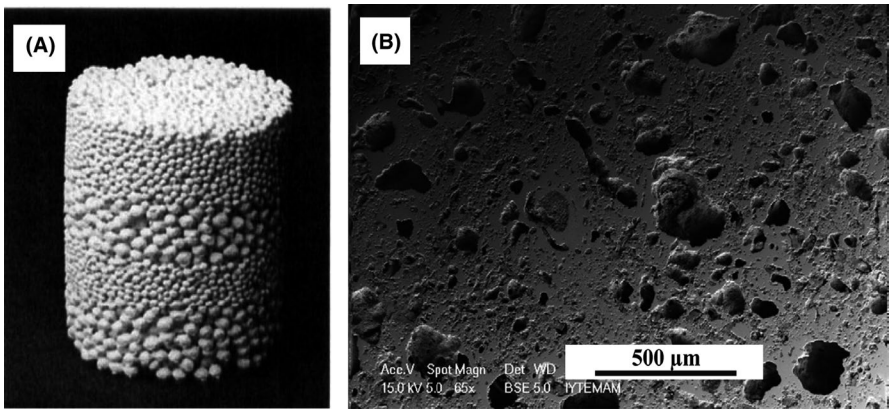

FIGURE 3 (A) Ceramic foam made by using peas and seeds as sacrificial templating with various diameters (Reproduced from[18] with permission John Wiley and Sons, Copyright 2004), (B) polished surface SEM image of an aluminum silicate sample made by using 30 wt% paper processing residue, and sintered at 1300°C (Reproduced from[19] with permission Elsevier, Copyright 2010)

TABLE 2 Properties of the closed porosity ceramics and glasses produced by high-temperature bonding

Formed ceramic or glass/pore-forming agent	Porosity	Pore size	Mechanical property	Other properties	Ref.
Alumina/Hollow alumina microspheres	ϕ_T ~ 63%		σ_c = 12 MPa		26
Alumina & mullite & borosilicate glass/hollow borosilicate glass microspheres	ϕ_T = 33%-36%		σ_{bs} = 105 MPa (@34% ϕ_T)	ε = 5.1	28
Borosilicate glass/hollow borosilicate microspheres	ϕ_T = 30%-35%				25
Mullite/quartz and fly-ash floating bead particles	ϕ_T ~ 44%-66% (~ 29%-31% ϕ_C)		σ_c ~ 105.5 MPa (@~44% ϕ_T)		27
Soda-lime-borosilicate glass/hollow soda-lime-borosilicate glass microspheres	ϕ_T ~ 82%-98%		σ_c ~ 15 MPa σ_{bs} ~ 0.8 MPa E ~ 1 GPa (@92% ϕ_T)		24
Sodium borosilicate glass/sodium borosilicate hollow microspheres	ϕ_T ~ 76%-92%		σ_{bs} = 7 MPa (@77% ϕ_T)		23

Note: ϕ_T = total porosity, ϕ_C = closed porosity, porosity calculations were done via Archimedes by using water or gas pycnometer & bulk density, σ_c = compressive strength, σ_{bs} = bending strength, E = Young's modulus, ε = dielectric constant.

2.2 | High-temperature bonding of hollow structures

Basically, in the process, hollow objects of the material to be produced (both as matrix and pore-forming agent) are fused at high temperature. There is no sacrificial agent but instead the raw materials create the final C&G with or without the aid of an additional high-temperature binder. Table 2 gives some properties of the closed porosity ceramics produced by high-temperature bonding and a simplified schematic demonstration of the process is given in Figure 4.

In the pioneering study conducted by D. J. Green[23] hollow-sodium borosilicate glass spheres (sieved below 75 µm) were used to fabricate closed pore, lightweight ceramics. Even at relatively low-sintering temperature, the fused beads were formed, the neck formation can be seen from the SEM images given in Figure 5A,B.[24] In a variant approach, hollow glass microspheres were mixed with glass powder and compacted in

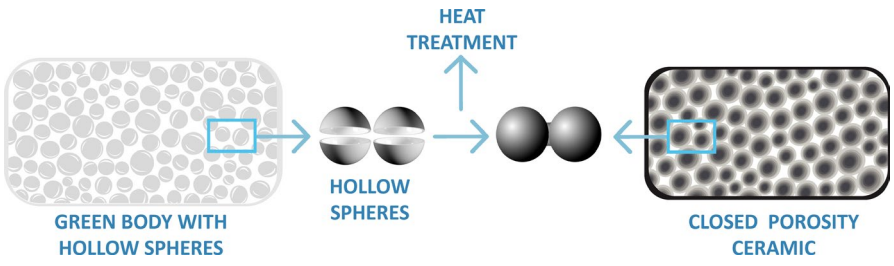

FIGURE 4 Schematic illustration of high-temperature bonding technique

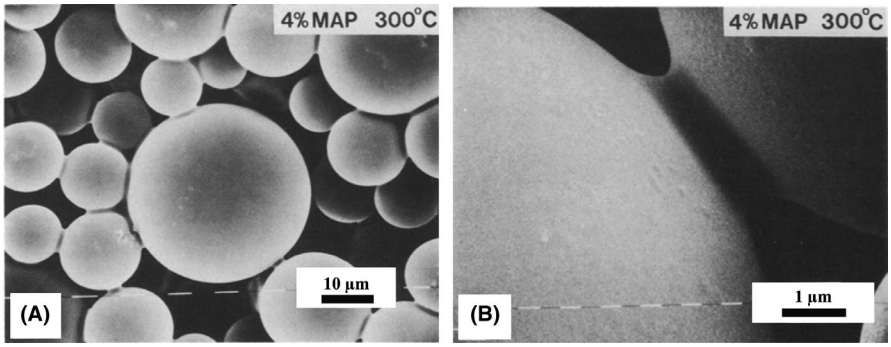

FIGURE 5 SEM micrographs of (A) soda-lime glass microspheres, bonded with 4 wt% mono-aluminum phosphate and fired at 300°C for 3 h, (B) close magnification demonstrating the neck formation (Reproduced from[24] with permission Springer Nature, Copyright 1985)

graphite die by hot-pressing under N_2 atmosphere, successive sintering in between 580°C and 620°C at 1.5 to 10 MPa pressure resulted in the closed porosities reaching up to 35%. Under the effect of uniaxial pressure during densification, the hollow beads were deformed by viscous flow, resulting in spheroidal shaped pores throughout the glass matrix.[25] In another study, not a phase-pure but closed-cell (ϕ_T = 63%) alumina ceramics were also made by using hollow alumina spheres having 200-2000 μm diameter together with B_2O_3 as flux, silica as high-temperature fusing agent, and mullite fibers as mechanical property enhancer.[26] Analogously, closed porosity (30%) mullite ceramics were formed from the mixture of quartz and fly ash beads. During the process, the formed SiO_2-rich transient liquid phase both led to pore isolation and accelerated the crystallization causing mullite crystallization on the cell walls.[27]

Probably the simplest technique for producing closed porosity C&Gs is based on the high-temperature bonding of the hollow structures (generally spheres). The contact points are glued at high temperatures resulting in the struts with reduced defects. The technique, which is suitable for porous structures with a high-porosity range between ~ 30 and 95%, is limited by the availability of the starting hollow structures. Indeed, it is mainly reported for processing of porous glasses starting from hollow glass spheres. Another problem may arise when the mixture is unable to cause adequate viscous behavior and additional high-temperature binder is added as fusing agent which eventually may causes a purity loss.

2.3 | Casting: gel casting and others

Casting, especially gel casting is a convenient way of obtaining porous C&Gs state with porosities reaching above 90%. For gel casting, basically a ceramic suspension consisting of foaming agent and water-soluble monomers is mixed, followed by gelation via polymerization (cross-linking) of the monomers, making the foamed structure stiff and able to resist the stresses during drying.[29] In general, the successive heat treatment results in highly porous ceramics with spherical pores and dense struts,[30] Table 3 documents the components produced by casting together with their properties. This hybrid casting route (principally it is a hybrid of traditional slip casting and polymer chemistry) is typically used to obtain permeable components but has also been modified to facilitate closed pore C&G artifacts when hollow structures (generally micron-sized spheres) are used as pore-forming agent, see Figure 6 for the schematic view for the gel-casting route. If hollow C&G microspheres are used within a ceramic slurry/gel having a different chemical composition, the final material is a multiphasic ceramic, that is ceramic matrix composite (CMC), which can be called as *ceramic syntactic foam* (see later).[31]

Coal ash (fly and bottom) is obtained from the coal combustion in thermal power plants as a by-product. While fly ash has been the subject of several studies, due to inherent chemical heterogeneity and course nature, limited number of studies have been conducted by bottom ash.[32] Fly ash is a rich source of hollow spherical (commonly < 500 μm in diameter) particles known as *cenospheres* (fly ash cenospheres, FAC).[33,34] Although their concentration in fly ash is relatively low (~1%), considering the amount of annual fly ash production globally (>365 million tons[35]), the overall amount of FAC is worthwhile to consider for the formation of closed porosity components.[36,37] In this regard, silica-based monoliths were formed by using FAC via gel-casting route.[38] Huo et al[39] used hollow fly ash spheres for the production of closed porosity mullite ceramics with a ϕ_T ~ 80. In other studies, closed porosity (<39%) silica using hollow silica spheres (see Figure 7A-D)[40] and borosilicate (ϕ_T ~ 56%-79%) using soda lime borosilicate, 40 μm diameter beads were also formed.[41] Other compositions such as alumina, zirconia, Si_3N_4/Si_2N_2O, etc were also produced by gel casting using environmental-friendly biopolymers (gelatin, ovalbumin (egg white), bovine serum albumin, chitosan, starch, alginate, agar, etc) instead of toxic monomers.[29,42–44] The resulting components usually had mixed pore type (open & closed) but characteristically having spherical cells interconnected by narrow circular windows, that is resembling those of closed porosity components when properties are considered.[42–47]

It is important to note that gel casting is a different process than sol-gel in which ceramic precursors are integral to the gelling process via hydrolysis, polycondensation, etc[48] While many studies were focused on gel casting, few others investigated the preparation of a sol-gel to cast[49,50] and gelation freezing.[51] Although, gel casting is facile and flexible technique to produce a wide variety of geometries and can be adapted to traditional

TABLE 3 Properties of the closed porosity ceramics and glasses produced by casting

Formed ceramic or glass/gelling & pore-forming agent(s)	Porosity	Pore size	Mechanical property	Other properties	Ref.
Alumina/agar & surfactants		50-800 μm			43
Alumina/agarose & surfactants	ϕ_T ~ 60%-89%	119-624 μm		λ = 0.48-0.74 W/m.K. (@89% ϕ_T)	42
Alumina/gelatin & soybean oil	ϕ_T ~ 64%-66% (~13%-49% ϕ_C)	~4-39 μm	σ_c ~ 15-62 MPa		47
Alumina/NMAM and MBAM & SDBS	ϕ_T ~ 43%-57% (~36%-52% ϕ_C)	~15-200 μm	σ_c = 23-41 MPa		46
Foam glass (borosilicate)/ACM and MBAM & hollow glass microspheres	ϕ_T ~ 56%-79%		σ_c = 2.8-17.1 MPa	λ = 0.07-0.16 W/m.K.	41
Clay-based/cenospheres	ϕ_T < 60%		σ_c = 26 MPa (@60% ϕ_T)		31
Mullite/ACM and MBAM & cenospheres	ϕ_T = 73%-81%		σ_c = 4.4-33.4 MPa		39
Multiphase ceramic & glass (combeite & hydroxyapatite-based)/anionic and nonionic surfactant mixture	ϕ_T ~ 85%-94%	~200-1000 μm	σ_c ~ 0.4-2.2 MPa		49
Silica/ACM and MBAM & cenospheres	ϕ_T = 37%-63% (23%-55% ϕ_C)		σ_{bs} = 14.5 MPa (@55% ϕ_C)	SSA = 69.32-106.52 m^2/g	38
Silica/ACM and MBAM & hollow silica microspheres	ϕ_T = 74%-80% (35%-39% ϕ_C)		σ_c = 3.2-14 MPa	λ ~ 0.102-0.218 W/m.K.	40
Silicon nitride-silicon oxynitride/agarose & cenospheres	ϕ_T ~ 62%-67%	14.40-16.60 μm	σ_{bs} = 21-39 MPa		45

Note: ϕ_T = total porosity, ϕ_C = closed porosity, porosity calculations were done via Archimedes by using water or gas pycnometer & bulk density, σ_c = compressive strength, σ_{bs} = bending strength, λ = thermal conductivity, SSA = specific surface area.

ceramic forming industry with no requirement of new instrumentation, the method uses high number of noneconomic and environmentally unfriendly chemicals. Besides, the used monomers are generally heavily toxic, drying period is long and large volumetric shrinkage occurs during firing. It is also useful to note that when hollow structures are used, the pore size/shape of the formed component is dictated by the initial pore characteristics of the hollow bodies.

2.4 | Direct foaming

Direct foaming is an economical, simple, and scalable technique used for the production of porous ceramic components by the dispersion of gas bubbles created via external insertion (blowing agents) or gas generation (self) through a liquid phase or a ceramic slurry. Different processing approaches are possible to create gas bubbles, and here they are categorized into two basic types, namely blowing agents and self-blowing. Figure 8 demonstrates a simplified schematic diagram for all direct foaming types.

2.4.1 | Blowing agents

Blowing agents are substances which are deliberately added to a mixture (polymeric, ceramic, etc) to produce gas and eventually create a porous component. General desirable properties of blowing agents can be summarized as: minimum ozone

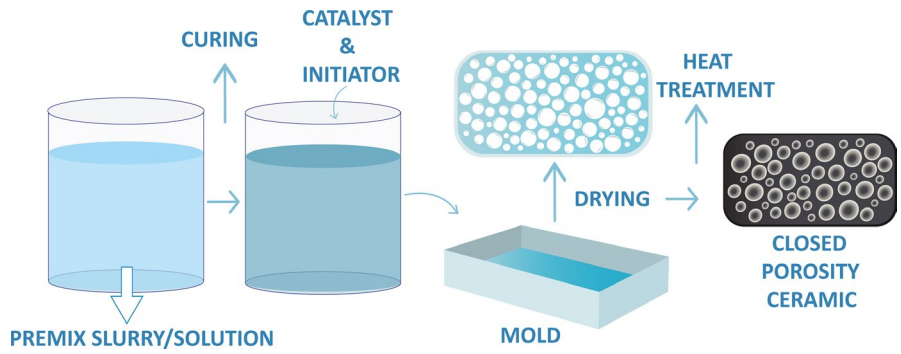

FIGURE 6 Schematic illustration of gel-casting technique

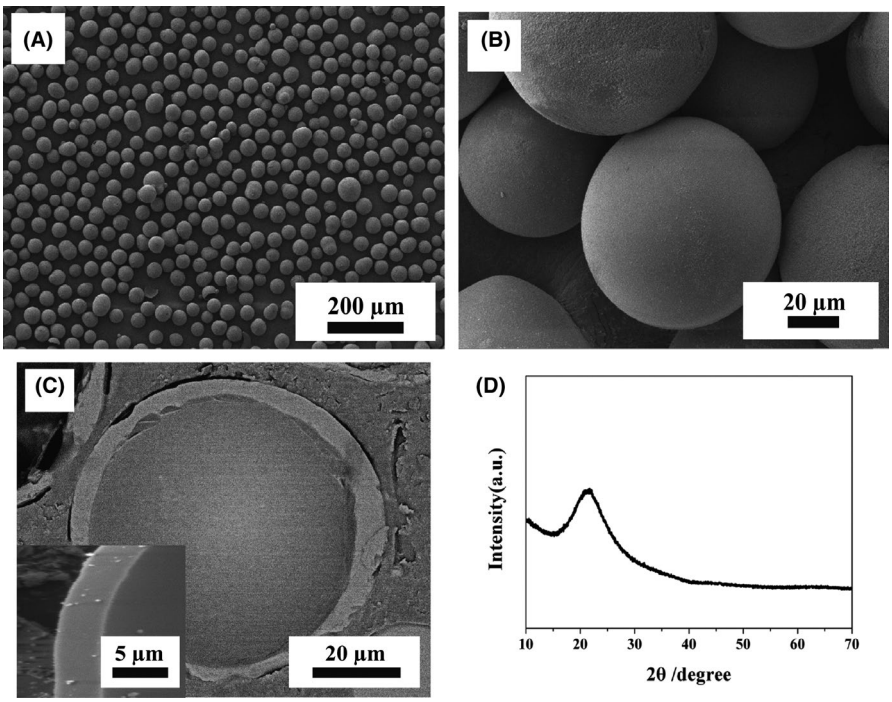

FIGURE 7 (A-C), SEM images of hollow silica spheres, in (C) the lower left inset shows the wall detail of the hollow structure, and (D) XRD pattern obtained from the spheres showing the amorphous nature (Reproduced from[40] with permission Elsevier, Copyright 2016)

depletion and global warming potential, decent storage stability, facile control (time/temperature) of gas release, low toxicity and odor during decomposition, nonflammable, ability to form uniform and stable cells, low-boiling point, and finally economic and readily available.[52] Blowing agents are analyzed into two basic types, namely physical blowing agents (PBAs) and chemical blowing agents (CBAs). While CBAs generate the desired gas by self-decomposition (thermal) or from the result of reaction with other compounds, for PBAs the origin of the created gas is different since there is no thermal decomposition or chemical reaction of the used agent.

Physical blowing agents

When a PBA is used, the aimed gas to blow the system is generated merely from the following physical changes: (a) volatilization (eg, phase change) of the compound(s), (b) desorption of primarily dissolved gases under high pressure, and (c) direct utilization of compressed gases (N_2, CO_2, etc).[52] Table 4 gives some properties of the closed porosity C&Gs produced by using different types of PBAs.

Pentane was used to produce closed porosity ($\phi_T = 85\%$) zirconium carbide (ZrC) ceramics (see Figure 9A,B with excellent thermal stability.[53] A typical foaming process was followed by using zirconia sol (zirconium oxychloride-water/ethanol-hydrogen peroxide), pentane, phenolic resin, Tween 20 as emulsifiers and citric acid as curing agent. Not only pentane but also other types of hydrocarbons (heptane, hexane isomers) can be used as PBA. These hydrocarbons, generally, are liquid at room temperature (RT) with boiling points below ~ 100°C. Gas desorption or solid-state foaming

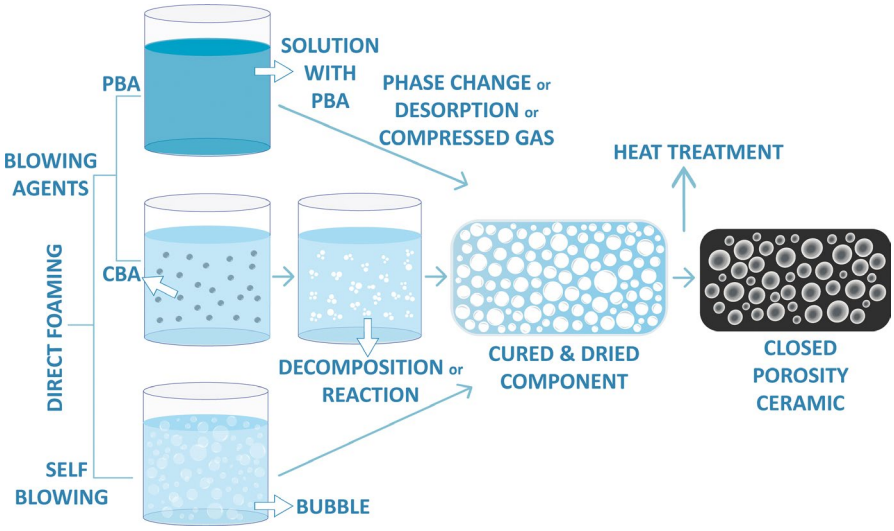

FIGURE 8 Schematic illustration of direct foaming technique

TABLE 4 Properties of the closed porosity ceramics and glasses produced by using physical blowing agents

Formed ceramic or glass/pore-forming agent	Porosity	Pore size	Mechanical property	Other properties	Ref.
Foam glass (Si-B-Na-based; borosilicate pyrex glass made)/argon	ϕ_T = 62%-80%	0.03-8 μm 50-70 μm	σ_c = 15-52 MPa E = 4.1-12.6 GPa		54
Foam glass (Si-Na-Ba-based; Cathode ray tube (CRT) waste glass made)/argon & helium & nitrogen	ϕ_T = 30%-89% (~30%-89% ϕ_C)				61
Cementitious foam (Portland limestone cement made)/Methyl cellulose & carrageenan gum & water	ϕ_T ~ 71%-94%	500-1000 μm	σ_c ~ 0.4 MPa σ_{bs} < 1 MPa	λ = 0.11 W/m.K. (@92% ϕ_T)	62
Multiphase ceramic (Kaoline-based; clay made)/methylcellulos & water	ϕ_T ~ 95%	5-400 μm	σ_c = 0.04-0.23 MPa E = 0.4-2.1 MPa	λ = 0.054-0.120 W/m.K.	63
Silicon carbide/carbon dioxide	ϕ_T = 45%	<10 μm			59,60
Silicon oxycarbide/carbon dioxide	ϕ_T = 64%-89%	50-400 & <20 μm	σ_c = 9 MPa E = 7 GPa		55–58
Zirconium carbide/pentane	ϕ_T ~ 68%-93%	40 μm	σ_c ~ 0.2-04 MPa	λ = 0.94 W/m.K.	50,53

Note: ϕ_T = total porosity, ϕ_C = closed porosity, porosity calculations were done via Archimedes by using water or gas pycnometer & bulk density, σ_c = compressive strength, σ_{bs} = bending strength, E = Young's modulus, λ = thermal conductivity.

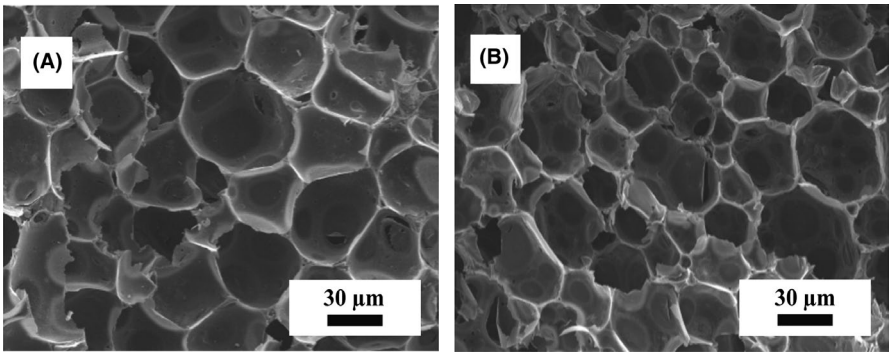

FIGURE 9 SEM images of ZrC foams after sintering at (A) 2200°C for 1 h and (B) 2400°C for 10 min in Ar atmosphere (Reproduced from[53] with permission Elsevier, Copyright 2014)

is another PBA method in which ceramic or glass powder is commonly consolidated under high-gas pressure (eg, by hot isostatic pressing under Ar at elevated temperatures) followed by desorption/expansion of the dissolved gas.[54] The last PBA technique is the compressed gas injection. For now, it was performed only on the preceramic polymers (PPs) in which the gas solubility and the molecule size (the small molecule diffuses much faster) in the liquid system found to be effective for final pore characteristics.[55–58] In a basic description, PPs were first saturated by CO_2, followed by heating and/or rapid pressure drop initiating foaming and finally pyrolysis at high temperature resulting in the microcellular ceramic.[55,59,60] The process was also adapted to a technical scale, that is extrusion coupled with simultaneous foaming by dissolved CO_2, and obtain diverse-shaped closed porosity polymer-derived ceramics (PDCs).[56–58]

Chemical blowing agents

Human beings have been using CBAs (in this case biological blowing agents, leavening agents) for thousands of years to obtain closed (or partially closed) porosity solid material, undoubtedly known as bread.[70] When wheat flour is hydrated, yeast and bacteria begin to process (ferment) producing alcohol, organic acids, and CO_2 gas which retain in the viscoelastic gluten network during both fermentation and baking.[71] In materials science, CBAs produce gas by thermal decomposition and/or by chemical reaction(s) with other components. Table 5 gives the list for components, their properties, and the CBA types. As one can see, oxidation of carbon, reduction/oxidation of carbide or nitride components, decomposition of carbonates and phosphates has been investigated extensively.

Kishimoto and his colleagues[72–80] followed solid-state (or superplastic) foaming by using various high temperature CBAs (SiC, Si_3N_3, AlN, etc). The reduction and/or active oxidation of these additives (see reactions 1-3 for SiC) during prolonged sintering of the superplastic matrix causes foaming. In this simple method, few percent (generally below 10 wt%) of foaming agent was coated or mixed with the target composition, pressed and sintered for extended periods (eg, 8 hours) at elevated temperatures. While the process does not yield with highly porous samples (ϕ_T was generally below 40%),

PANEL I: Solid-state foaming/thermodynamic instability

Solid-state foaming technique has long been used to produce porous metallic materials having high-melting temperatures. Initially metal powder is consolidated under gas pressure (generally Ar) by hot isostatic pressing (HIP). The obtained billet after HIP has relatively low porosity (<1%) constituted by highly pressurized gas used during the process. At medium/high-heat treatment temperatures (isothermal) foaming proceeds via creep of the metal matrix surrounding the pores, in other words initially gas-pressurized pores expand by isothermal creep.[64,65] However, under isothermal conditions creep rate is low, so even with extensive heat treatment periods (>100 hours) insignificant total porosities usually below 30% were obtained. Alternatively, it was shown that thermal cycling about the allotropic temperatures can induce simultaneous creep and transformation-superplasticity operational conditions enhancing the matrix deformation around the gas-filled pores. In this way an improvement was obtained both in foaming rates and porosities reaching to 44%.[66,67]

Inspired by the above, Wang et al[54] fabricated closed porosity borosilicate monoliths. First, borosilicate powder was melted (1100°C/1h) by capsule-free HIP from under 10 to 70 MPa Ar pressures. At this stage, Ar was not only entrapped (note that the glass matrix at this stage was having high-relative density > 95%) but also it was dissolved in the network (at high HIP pressures). Isothermal heat treatment at 800°C for 10 min caused an expansion of Ar-filled pores by an ample viscous flow of the glass matrix, together with the release of the dissolved Ar leading to the formation of micron-sized small pores. The porous borosilicate samples having a ϕ_T ~ 80% were formed in this way.

Solid-state foaming process was also employed on polymeric materials (foaming around or above glass transition but below the melting temperature of the neat polymer to obtain microcellular structures.[68,69] Simply, it involves the following steps: (a) saturating the polymer with nonreactive gas, (b) heating the polymer to softening point (glass transition temperature), (c) reducing the ambient pressure to induce the gas nucleation from super-saturated state, (iv) rapidly cooling the polymer to prevent the cell growth, whereby cells sizes about 2 to 25 μm can be obtained. Since basically transition from an unstable to a stable thermodynamic state is causing the cell nucleation from super-saturated polymer, it is also called as *thermodynamic instability* technique. The thermodynamic instability principle is followed by using PPs to produce ceramic artifacts with closed porosity. Figure 10 depicts the proposed mechanism, for more details the interested reader is referred to a recent review on the porous PDCs.[1]

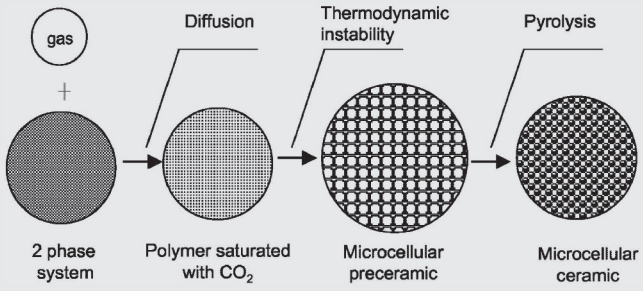

FIGURE 10 Processing of preceramic polymers with CO_2 system to obtain closed-cell microcellular ceramic. Note that to form two phase system, instead of gas supercritical or liquid state can also be used (Reproduced from[59] with permission John Wiley and Sons, Copyright 2003)

yttria-stabilized zirconia (3YSZ and 8YSZ), alumina (with superplasticity-facilitating dispersoids; 3YSZ, 0YZ or spinel) and titania-based closed porosity ceramics were produced.[72–80] Similarly, recycled materials (eg, granite scrap and fired clay tailings) were used with SiC to cause gas generation and form closed porosity ceramic foams.[81] In a different technique, closed porosity aluminum oxynitride (AlON) (ϕ_C = 80%) foams were made by combustion synthesis in between 2165°C and 2650°C for a very short time (10 seconds). Al and Al_2O_3 were reacted under high (100 MPa) N_2 pressure together with $Al(NO_3)_3.9H_2O$ which was used as high-temperature decomposing pore-forming agent yielding AlON foams.[82] Besides, inspired from aerated concrete (AC) production methods,[83] closed porosity (<74%) multiphase ceramics were fabricated by using alkali activated fly ash and Al powder reacting to release H_2 gas as a pore former.[84]

$$SiC + O_2(g) \rightarrow SiO + CO(g), \quad (1)$$

$$SiC(s) + 3/2O_2(g) \rightarrow SiO_2 + CO(g), \quad (2)$$

$$SiC(s) + 2SiO_2(s) \rightarrow 3SiO(g) + CO(g). \quad (3)$$

TABLE 5 Properties of the closed porosity ceramics and glasses produced by using chemical blowing agents

Formed ceramic or glass/pore-forming agent	Porosity	Pore size	Mechanical property	Other properties	Ref.
Aluminum oxynitride/aluminum nitrate hydrate	ϕ_T ~ 60%-80%[a] (~80% ϕ_C)	0.1-1500 μm			82
Alumina & Zirconia/aluminum nitride & boron nitride & silicon carbide & silicon nitride	ϕ_T ~ 25%-57%	4.24-2000 μm	σ_{bs} ~ 10-520 MPa	ε ~ 5.5-8 λ ~ 1-4.5 W/m.K.	72–76,79
Multiphase ceramic (Hauyne-based; red mud & fly ash made)/ Sodium silicate	ϕ_T ~ 64%-74%	1-3 mm & 100-500 μm	σ_c, = 4-10 MPa		86
Fly ash[¥]/aluminum	ϕ_T = 50%-74%		σ_c = 6 MPa σ_{bs} = 1 MPa (@61.7% ϕ_T)	λ = 0.145 W/m.K.	84
Multiphase ceramic (Quartz-based; granite scrap & clay made)/ silicon carbide	ϕ_T ~ 83%	2000-5000 μm	σ_c = 0.9 MPa σ_{bs} = 0.4 MPa	λ = 0.051 W/m.K.	81
Porcelain/silicon carbide, calcium oxide & calcium sulfate	ϕ_T ~ 47%-90%	<570 μm	σ_c ~ 2-15 MPa		87
Stoneware/calcium carbonate	ϕ_T ~ 26%-36%	<30 μm ~ 200 μm	E ~ 40-70 GPa		88
Zirconia/P-O gas species	ϕ_T ~ 27% (~25% ϕ_C)	5-20 μm	σ_{bs} = 200 MPa		89,90
CBAs for foam glasses & glass-ceramics					
Foam glass (Si-Na-Ca waste glass & fly ash made)/Silicon carbide	ϕ_T ~ 82%		σ_c = 1 MPa		91
Foam glass (Si-Na-Ca waste glass & fly ash made)/silicon carbide	ϕ_T ~ 86%-93%		σ_c = 0.9-1.8 MPa		92
Foam glass (Si-Na-Ca waste & alumino-silicate glass made)/ Silicon carbide	ϕ_T ~ 88%-92%	1000-4000 μm	σ_c = 0.5-2.6 MPa		93
Foam glass (SiO_2, Al_2O_3, R_2O, B_2O_3, Sb_2O_3 made)/carbon black	ϕ_T ~ 80%	500-1300 μm			94
Foam glass (Si-Na-Ca waste glass made)/Sodium water-glass & water	ϕ_T ~ 43%-84%	4 nm−800 μm		λ = 0.14 W/m.K. (@84% ϕ_{TP})	95
Foam glass (Si-Na-Ca waste glass made)/propyl gallate	ϕ_T ~ 91%-97%		σ_c = 0.3-5.9 MPa	λ = 0.055-0.077 W/m.K.	96,97
Glass ceramic foam (wollastonite-based; Si-Na-Ca waste glass & coal pond ash made)/silicon carbide	ϕ_T = 70%-90%	60-3000 μm	σ_c ~ 1.5 MPa (@~75% ϕ_T)		98
Glass ceramic foam (diopside-based; CRT waste glass & germanium tailings made)/silicon carbide		200-1500 μm	σ_{bs} ~ 3.3 MPa	λ = 0.68 W/m.K.	99
Glass ceramic foam (Pb-O, Al-Si-based; CRT waste glass made)/ silicon carbide		500-2500 μm	σ_c ~ 12-24 MPa σ_{bs} ~ 5-16 MPa		100
Glass ceramic foam (quartz-based; coal gangue & sand made)/ calcium carbonate	ϕ_T ~ 70%-73%		σ_{bs} = 4.5-6 MPa		101
Glass ceramic foam (diopside-based; fly ash & Si-Na-Ca waste glass made)/calcium carbonate	ϕ_T = 79%	200-1500 μm	σ_c = 5.2 MPa	λ = 0.36 W/m.K.	102
Glass ceramic foam (quartz-based; red mud & coal gangue made)/Calcium carbonate	ϕ_T ~ 40%-88%	~280-630 μm	σ_c = 6.5-17.8 MPa σ_{bs} = 3.1-10.1 MPa	λ ~ 0.09-0.10 W/m.K.	103
Glass ceramic foam (devitrite-based; CRT & flat & window & container glass made)/calcium carbonate, carbon, iron oxide, manganese oxides	ϕ_T ~ 41%-94% (~ 3%-95% ϕ_C)	~20-4000 μm	σ_c = 0.5 MPa	λ = 0.038-0.075 W/m.K.	104–109
Glass ceramic foam (silica-based; Si-Na-Ca glass made)/aluminum nitride	ϕ_T ~ 53%-88%				110
Glass ceramic foam (quartz-based; quartz & calcium carbonate & talc made)/silicon nitride	ϕ_T = 38%-89% (11%-88% ϕ_C)		σ_c = 3.3-37.4 MPa		111
Glass ceramic foam (silica-based; Si-Na-Ca waste glass made)/ sodium hydroxide	ϕ_T ~ 86% (~ 79% ϕ_C)	16-744 μm			112
Glass ceramic foam (Na-Al silicate based; fly ash made)/sodium silicate	ϕ_T ~ 55%-69%		σ_c = 2.6-10.5 MPa σ_{bs} = 1.4-6.6 MPa		113
Glass ceramic foam (cristobalite-based; Si-Na-Ca-B waste glass made)/organic binder	ϕ_T ~ 68%-80%	10-300 μm			114

Note: ϕ_T = total porosity, ϕ_C = closed porosity, porosity calculations were done via Archimedes by using water or gas pycnometer & bulk density, σ_c = compressive strength, σ_{bs} = bending strength, E = Young's modulus, ε = dielectric constant, λ = thermal conductivity, ¥ = not specified.

[a]Calculated.

PANEL II: Foam glass & glass ceramics

Foam glass possesses high-specific strength, low-thermal conductivity, high freeze-thaw tolerance & chemical inertness, nonflammable, and nontoxic behavior. It can be produced from readily available economic-raw materials, for example waste glass; besides, generally it has a long service life (>100 years). Such issues make it one of the most useful source especially for construction industry[115,116] where the application temperatures are normally far below 500°C, that is under the softening temperature of the glass matrix. The details for the formation of foam glass can be found in Prof. Scarinci's comprehensive chapter,[116] here aside from the properties of the most recent works documented in Tables 4–6, only a brief overview for few compositions will be mentioned.

Traditionally, foam glass is produced by grind-mix, pack and heat treatment procedure. The glass powder (usually recycled waste glass) is mixed with "gasifier" which is basically a CBA (PBAs or self-foaming blends are also possible) and heat treated above the softening (Littleton) temperature. This procedure provides a certain viscosity level at which the decomposition of the foaming agent generates bubbles, remaining as isolated pores in the solidified body upon cooling. CBAs used for the foam glass production can be summarized as: (a) decomposition of carbonates (usually $CaCO_3$), (b) reduction/active oxidation of carbon/carbide/nitrides (usually SiC), and (c) redox reactions of transition metal oxides (usually Fe_2O_3)[108,117] see Table 5 for the details. It should be noted here that by definition glass ceramics are above 50 vol% crystalline and for the applications, crystallinity higher than 90 vol% is usually demanded.[118] Since in several papers summarized in Tables 4–6, most of the time there was no proper phase quantification or the samples had low crystallinity levels, probably *glass ceramic* term was inaccurately used. However, appropriate identification of these components is not possible and therefore the same terminology will be followed. If the produced component is a mixture of amorphous and crystalline phases, it is called "glass ceramic foam" underlining also the main crystal precipitate.

The selection of suitable foaming agent is directly related to the viscosity of the glass. Heating rate, temperature and dwell time, the particle size of both foaming agent and glass powder (generally fineness below 400 μm) are critically important parameters for successful foaming. The viscosity usually used for hot drawing operations, that is above Littleton temperature and in between 10^5 and 10^3 Pa.s., is the most suitable to enhance the porosity.[116] The type of forming agent can also influence the viscosity of the blend, for example alkali carbonates or phosphates can further reduce the viscosity because of alkali introduction into the glass network.[108]

Besides waste glass, different recycled or natural materials (granite scrap and fired clay residue),[81] ashes (fly, volcanic or sewage sludge), various types of slags and mine/mill tailings[91–93,98–100] were used with few amounts of additional silicon carbide (<10 wt%) releasing gas species at high temperature, see Equations 1-3.[119] In this way, it was possible to obtain closed porosity foam glass with $\phi_T = 82\%$ (calculated via bulk density measured by geometric evaluation) and 1 MPa compressive strength,[91] or glass ceramic foam with wollastonite-diopside crystals having $\phi_T = 90\%$ and 2.6 MPa compressive strength,[93] see Figure 11 for representative samples.

A variant study was conducted by using carbon black to produce closed porosity borosilicate foam glass. The wet-mixed mixtures of SiO_2, Al_2O_3, B_2O_3, Sb_2O_3, other oxides and carbon black were heat-treated at 1400ºC/30 min. As known carbon black has oxidation temperature below 900ºC meaning that pre-oxidized carbon black was not the only pore former but

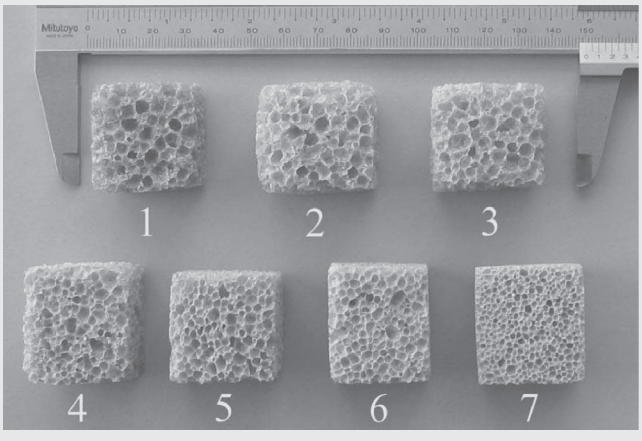

FIGURE 11 Photo demonstrating the macrostructure of the foamed glasses with altered pore size. These samples were obtained from the gas generation by using SiC foaming agent. While increasing the amount of foaming agent (1 to 3) did not change pore size, increasing the amount of alkali-earth glass (4-7), higher viscosity and smaller pore size was observed (Reproduced from[93] with permission Springer Nature, Copyright 2006)

probably also other high-temperature oxygen releasing additives such as Sb_2O_3, MnO_2, etc[94] Sodium silicate can also be used as a blowing agent. $Na_2O{\cdot}2.3SiO_2$, Na_2HPO_4 (stabilizer), $Na_2B_4O_7$ (flux), and fly ash were mixed, pressed into disk-shaped tablets, followed by sintering at 800°C/1h/air. The produced samples had variable total porosity (~55%-69%) and mechanical property values reaching to 10 MPa.[113]

In chemical blowing systems, the decomposition process can be exothermic or endothermic. Endothermic ones necessitate heat for decomposition maintenance; therefore, it is possible to control the decomposition and produce relatively small celled structures. Process control for exothermic CBAs is more difficult and generally results in large and nonuniform cell-sized products.[85] Unless the composition is low-temperature curable, CBAs necessitate the formation of viscous (glassy) phase to generate closed porosity C&Gs.

2.4.2 | Self-foaming

The distinction in between self-foaming and blowing agent usage is based on the fact that in self-foaming systems, there is no deliberate addition of an extra component to generate porosity, instead raw materials which will be used for the targeted ceramic composition induce gas evolution. This accounts also for the studies in which the gas generation is caused by (a) self-reactions of reagents, for example cross-linking/curing processes resulting in volatile by-products such as water, alcohol, etc (b) the release of physically/chemically bound water, and (c) the reactions of raw materials with each other. These works with the absence of intentionally added pore-forming agent are examined in this section, and the produced components, their properties are given in Table 6.

Closed porosity boron nitride (BN) monoliths were formed by the pyrolysis at 1500ºC/3h. Through curing which was conducted under different H_2 pressures, borazine precursor underwent condensation polymerization, releasing H_2 gas and foaming the matrix. It was found that increasing

TABLE 6 Properties of the closed porosity ceramics produced by self-foaming

Formed ceramic or glass/pore-forming agent	Porosity	Pore size	Mechanical property	Other properties	Ref.
Alumina/isopropyl chloride	ϕ_T ~ 94%-99%	50-300 μm		SSA = 265 m^2/g	127
Aluminum phosphate/gas¥	ϕ_T ~ 74%-91%[a]				126
Boron nitride/Hydrogen	ϕ_T ~ 88%-96%[a]	50-100 μm	σ_c ~ 4-8 MPa	ε = 1.25-1.55 λ = 0.03-0.05 W/m.K.	121
Foam glass (Borosilicate based: Si-B-Na-based Duran glass made)/gas¥	ϕ_T = 38%	5-50 μm			128
Foam glass (Si-Ca-Mg-S waste glass made)/Sulfur dioxide & oxygen	ϕ_T ~ 30%-68%	8-580 μm		λ = 0.115-1.113 W/m.K.	129
Mullite/Water & C-O gas species	ϕ_T ~ 81% (~52% ϕ_C)	850 μm	σ_c = 6.3 MPa		130
Glass ceramic foam (Andesine-based; Si-Na-Ca waste glass & basalt scoria made)/Oxygen	ϕ_T ~ 53%-86% (~ 8%-52% ϕ_C)	~25-1000 μm	σ_c ~ 2-50 MPa σ_{bs} ~ 11-17 MPa E ~ 19- 27 GPa		125
Multiphase ceramic (Hauyne & hematite based; fly ash/red mud made)/Sulfur dioxide & oxygen from LZTM	ϕ_T ~ 39%-80%	110-630 μm 350-4750 μm	σ_c = 3.6-26.4 MPa	λ = 0.21 W/m.K. (@76.2% ϕ_T)	120,122 123,124
Multiphase ceramic (nepheline based; CFA made)/Water	ϕ_T ~ 66%-84%	~300-1500 μm	σ_c = 8.3-13.9 MPa	λ = 0.098-0.198 W/m.K.	131
Silica/C-O gas species	ϕ_T ~ 39%-77%	~340 μm	σ_c ~ 0.6-29.8 MPa		132
Silica & silica/silicon nitride/water	ϕ_T = 60%-84%	10-120 μm	σ_{bs} = 9.7-16.3 MPa		133

Note: ϕ_T = total porosity, ϕ_C = closed porosity, porosity calculations were done via Archimedes by using water or gas pycnometer & bulk density, σ_c = compressive strength, σ_{bs} = bending strength, E = Young's modulus, SSA = specific surface area, ε = dielectric constant, λ = thermal conductivity, ¥ = not specified.

[a]Calculated from foam density using also theoretical density of dense component.

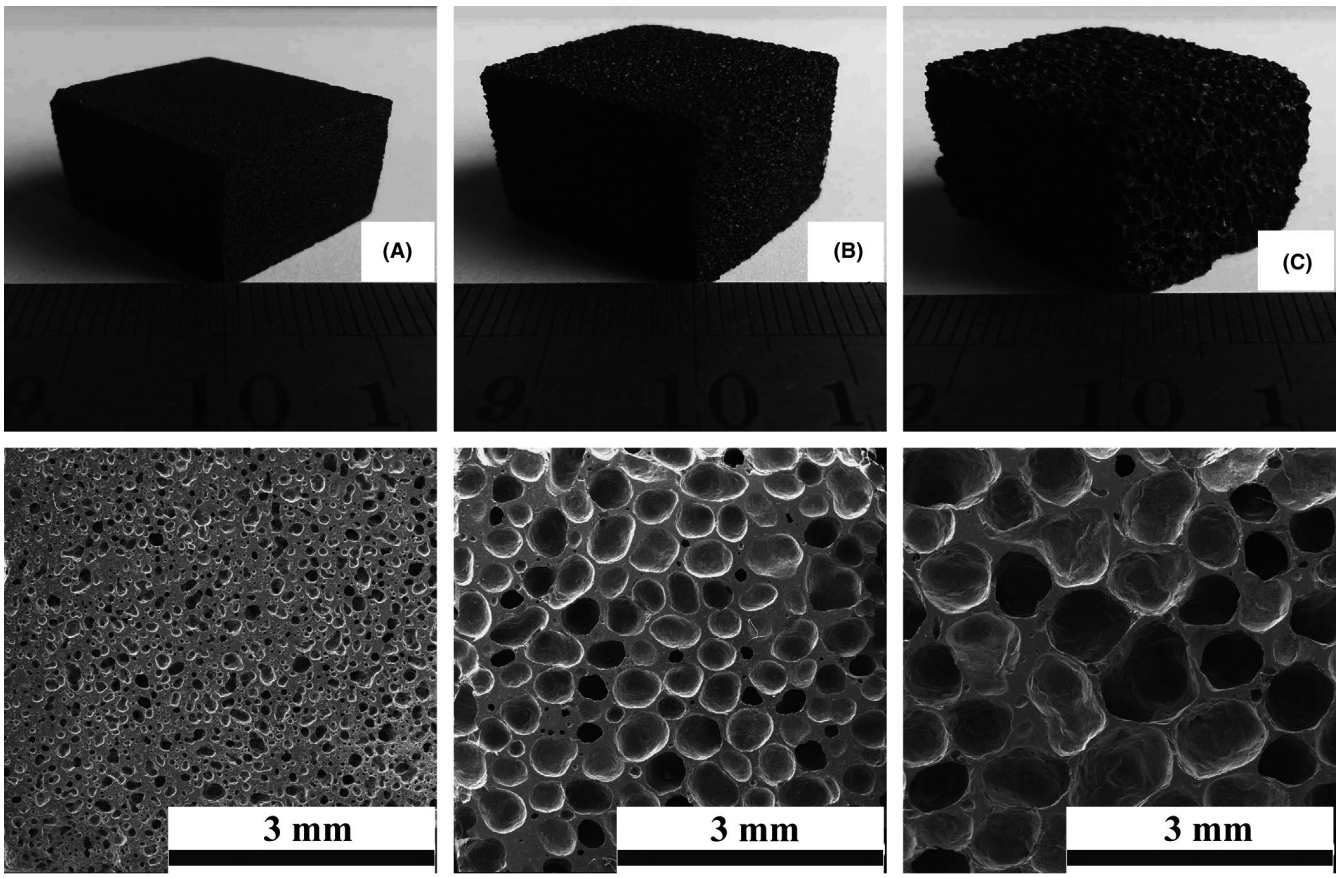

FIGURE 12 Digital photo images (top) and SEM images (bottom) of the samples sintered at temperatures: (A) 900°C, (B) 950°C, (C) 1000°C. (Reproduced from[120] with permission Elsevier, Copyright 2016)

the H_2 pressure, decreased the cell size and high total porosities reaching 96% could be obtained.[121] Lead-zinc mine tailings (LZMT) are hazardous wastes, originated during lead and zinc production. These tailings (constituted mainly by SiO_2, CaO, Fe_2O_3, and SO_3) and fly ash powder were mixed, pressed, and heat-treated. The authors claimed that various chemical reactions occurred through the heat treatment (eg, pyrite oxidation, de-sulfurization, etc) and these reactions created the gas bubbles which were enclosed by the viscous glassy phase solidifying finally as isolated pores Similar study was conducted by using red mud and silica instead of fly ash. The total porosity values for the formed multiphase ceramics were reaching around 80%, and it was shown that increasing the sintering temperature one could control the pore size by effecting the gas pressure and viscosity, see Figure12A-C for representative samples.[120,122–124] The redox reactions occurring between different iron oxide species were the reason for the formation of closed porosity multiphase ceramics obtained by sintering basalt scoria and soda lime cullet mixture.[125] Another simple approach was presented to obtain closed porosity aluminum phosphate foams by using aluminum hydroxide, phosphoric acid, and sodium hydroxide.[126] Heat treatment of aluminum chloride isopropyl ether complex $[AlCl_3(Pr^i_2O)]$ sols caused an initial precursor decomposition and the formation of alumina-based total porosity ($\phi_T = 99\%$).[127]

While direct foaming is facile and applicable to large-scale manufacturing (eg, no need to regulate templating agent decomposition), the control over the pore size and dimensionality in the final ceramic component is complicated. Besides, the reaction by-products remaining in the isolated pores, for example sulfur-based ones, can be hazardous.

2.5 | Emulsions

An emulsion is basically a suspension of one liquid into another immiscible liquid. Such instable mixture tends to separate into the phases constituting it, such as water and oil.[134] Traditionally emulsion stability is rescued by using surfactant molecules; however, other skills by liquid crystalline phases, interfacial reactions, asphaltene components and particle stabilization are also possible. For the last approach, stabilization is imposed by the localization of colloidal particles at the liquid/liquid interface, making them locked and thus inducing an extraordinary stability even at low particle concentrations.[134] Table 7 gives some properties of the closed porosity C&Gs produced by using emulsion technique.

Emulsion-forming strategy has already been explored for the formation of solid structures.[137–139] But specifically for the particle-stabilized systems, Gonzenbach et al[140] did the pioneering work and demonstrated the formation of stable wet foams by using short-chain amphiphiles adsorbed on the particle surface to stabilize high-particle concentration in the liquid phase. Following the wet foam (emulsion) synthesis, samples were dried, let for gelation, and finally sintered at 1575°C/2 h. The resulted closed porosity alumina ceramics had variable cell size, total porosity approaching 90% and high-compressive strength values reaching 16.3 MPa (at $\phi_T = 86.5\%$).[6,141] Studies of Garcia-Tunon et al[135] demonstrated that by altering the processing conditions one could obtain complex macroshaped ceramics having closed, open or graded porosity, see Figure 13A. It was shown that adjusting the solid loading, pH trigger, and applied energy, one might obtain closed porosity alumina ceramics with extraordinary compressive strengths above 300 MPa ($\phi_T = 55\%$). In a similar way, alumina, alumina-zirconia (see Figure 13B-E), ZTA, silica, kaolin-based, and Si_3N_4 ceramic foams with controllable microstructure (ie, open or closed porosity) were obtained merely by varying the processing conditions (surfactant or amphiphilic stabilization, composition, shearing conditions, etc) supporting the fruitfulness of the technique.[136,142–149] In a different approach, zirconia[150] and barium strontium titanate (BST, $Ba_{0.5}Sr_{0.5}TiO_3$)[151] ceramics were produced by using sodium dodecyl sulfate (SDS) surfactant as stabilizer both for zirconia (480 nm) and BST (550 nm) powders. For BSTs while ϕ_T remained below 95% (~46-100 μm cell size), for zirconia foams, porosity levels as high as 98% (50-150 μm cell size) were able to be reached.

The stability of the wet foam is challenging for emulsion systems, and as known it plays a major role in the final microstructural evolution. If such stability is ensured, the process is basically suitable for large scale, continuous manufacturing and could be specified as one of the unique method that allows precise control over the pore size and pore geometry together with complex geometric possibilities. However, still the method requires additional ingredients, energy input (to shear), and time increasing the cost.[152,153]

TABLE 7 Properties of the closed porosity ceramics and glasses produced by emulsion technique

Formed ceramic or glass	Porosity	Pore size	Mechanical property	Other properties	Ref.
Alumina	ϕ_T ~ 80%-89% ϕ_T ~ 79%-84%	24-35 μm 50-200 μm	σ_c = 11.8-22.9 MPa		141
Alumina	ϕ_T < 80%	30-300 μm			154
Alumina	ϕ_T ~ 95%-98%	50-200 μm	σ_c = 0.4-0.7 MPa (@96.7%-97.5% ϕ_T)		155
Alumina	ϕ_T ~ 50%-85%	~150 μm			149
Alumina	ϕ_T ~ 25%-89%	~ 20-140 μm	σ_{bs} ~ 5-42 MPa E ~ 4-50 GPa	λ = 3.3 W/m.K. (@~80% ϕ_T)	145
Alumina	ϕ_T ~ 80%	4-30 μm	σ_c > 300 MPa (@~55% ϕ_T)		135
Alumina-zirconia composite	ϕ_T ~ 96%-97%		σ_c ~ 0.6-1.5 MPa		136
Barium Strontium Titanate	ϕ_T = 81%-95%	46.40-100.40 μm		ε = 47-150	151
Kaolin	ϕ_T = 57%-95%		σ_c = 0.04-10 MPa E ~ 0.007-0.39 GPa	λ = 0.054-0.23 W/m.K.	146
Mullite	ϕ_T = 63%-79%	28-48 μm	σ_c ~ 27-71 MPa (@63%-75% ϕ_T)		156
Silica	ϕ_T ~ 45%-83% (~4%-33% ϕ_C)				142
Silicon nitride	ϕ_T ~ 40%	~10 μm	σ_{bs} = 106 MPa		144,148
Zirconia	ϕ_T = 96%-98%	50-150 μm	σ_c = 0.6-1.4 MPa (@96.5%-97.6% ϕ_T)	λ = 0.027 W/m.K. (@97.9% ϕ_T)	150
Zirconia-toughened alumina	ϕ_T = 88%-94%	0.54-1.26 μm 80-200 μm	σ_c = 8 MPa (@90% ϕ_T)		147

Note: ϕ_T = total porosity, ϕ_C = closed porosity, porosity calculations were done via Archimedes by using water or gas pycnometer & bulk density, σ_c = compressive strength, σ_{bs} = bending strength, E = Young's modulus, λ = thermal conductivity, ε = dielectric constant.

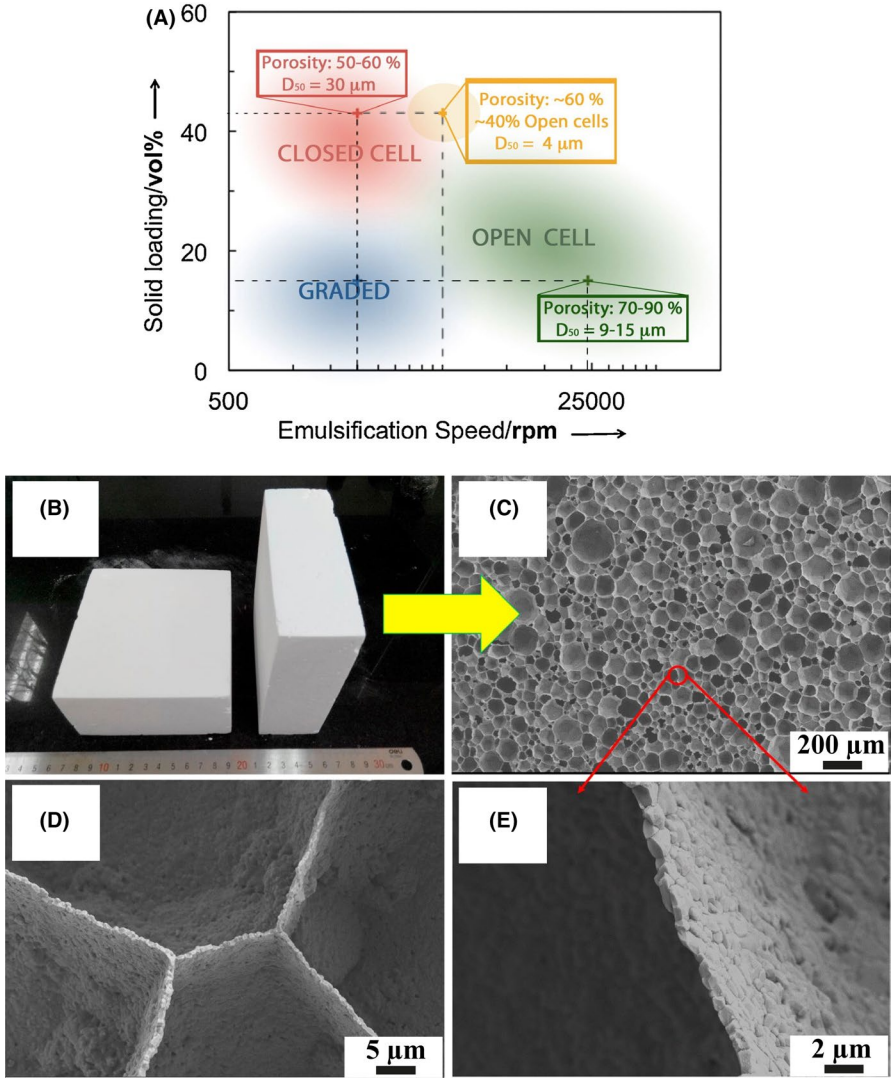

FIGURE 13 (A) Summary of particle-stabilized emulsion processing conditions to alter the final microstructure (Reproduced from[135] with permission Elsevier, Copyright 2017), (B) Image of bulk alumina/zirconia foam prepared from alumina-zirconia mixture with SDS surfactant by 1500°C sintering. SEM images showing (C) general view of closed porosity microstructure, (D) closed magnification view of polyhedral cells, and (E) thin strut detail (Reproduced from[136] with permission Elsevier, Copyright 2019)

3 | PROPERTIES AND APPLICATIONS

Closed porosity C&Gs are used in wide variety of industrial fields such as marine, aerospace, automotive, civil, etc The most important properties for these applications areas are detailed below.

3.1 | Mechanical behavior

For the mechanical behavior of porous materials, different models have been proposed;[157–160] however, ambiguity still remains especially for the closed-cell solid structures. Gibson and Ashby (GA) developed their theories by emphasizing on the solid matrix (strut/truss to lattice concept), instead another common one called *minimum solid area* (MSA) model proposed by Rice, focuses on the space holder that is pore, the details for such models are discussed extensively.[11,161–163] It is important to note that none of those models can properly be applied to all range of porosity levels. However, broadly speaking hardness and elastic modulus data fits more accurately than fracture toughness and strength which may vary considerably from the models.[160] In Figure 14, the compressive strength data collected from the published studies (if given) were plotted against the amount of porosity; the scatter can clearly be seen. The information which can be extracted from this plot is that the compressive strength is mainly dependent from the total porosity (ie, it decreases with the increase in the amount of porosity) while is difficult to correlate it with the process type used to fabricate the material. Indeed, as it will be shown later on, the amount of porosity is not the only parameter which can affect the strength but also pore topology and especially pore size.

Since GA model can be related to highly porous brittle solids, here it will be assumed as valid to investigate such scatter as well. Accordingly, the deformation behavior of porous ceramics can be interpreted from three dominating factors: (a) the cell shape (ie, lattice/truss topology), (b) the relative density, and (c) the properties of the solid matrix.[164] In view of these,

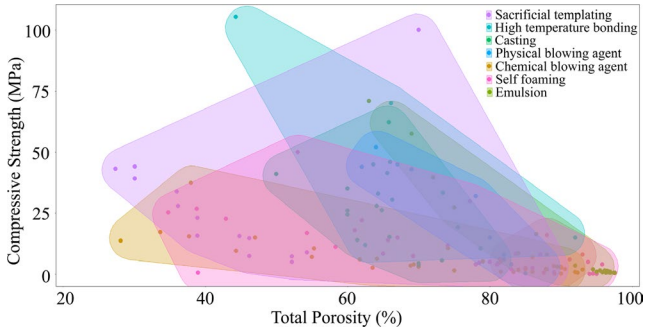

FIGURE 14 Compressive strength versus total porosity chart which was made by using RStudio software's Ggforce module with the data collected from the published papers

theoretical expression for compressive collapse strength (cold) which is the most investigated mechanical property for porous materials, is given in Equations (4) and (5) for open, and closed porosity brittle solids, respectively. In these expressions, σ_{cr} *is* crushing strength, σ_{fs} is the strut modulus of rupture, Φ is the solid material fraction in the cell edges, meaning that the remaining $(1-\Phi)$ is the material in the cell faces, and as claimed by Gibson and Ashby[161] when the fraction of the material in the cell faces increases, the strength dependence transfers from a power of 3/2 to a linear.

$$\frac{\sigma_{\mathrm{cr}}}{\sigma_{\mathrm{fs}}} = 0.2\left(\frac{\rho_{\mathrm{foam}}}{\rho_{\mathrm{skeleton}}}\right)^{3/2} \cdot (\text{open cells}), \tag{4}$$

$$\frac{\sigma_{\mathrm{cr}}}{\sigma_{\mathrm{fs}}} = 0.2\left(\Phi\frac{\rho_{\mathrm{foam}}}{\rho_{\mathrm{skeleton}}}\right)^{3/2} + (1-\Phi)\left(\frac{\rho_{\mathrm{foam}}}{\rho_{\mathrm{skeleton}}}\right) \cdot (\text{closed cells}). \tag{5}$$

It could be inferred from the modeling studies conducted on the metallic foams that the closed porosity structures (especially at low-relative densities) should have the enhanced mechanical properties compared to that of the open porous ones. This is because in the theoretical expressions for mechanical properties for close-cell foams—as can be seen above—additional correlations (eg, the contribution of cell faces) should be taken into account. In a study conducted for solid-state foaming of glass, it was also demonstrated that increasing the HIP pressure resulted in the enhancement of both the compressive strength (52 MPa) and the Young's modulus (12.6 GPa). The reason for the strength enhancement was explained by high-gas pressure in the pores reminiscent of superior collapse strength for the stalks/leaves having closed cells with the turgor pressure higher (for a freshly picked leaf ~ 6 atm) than atmospheric pressure.[161] Therefore, for a real approximation, the pressure of the entrapped gas in the isolated cells should also be considered in order to evaluate the complex mechanical behavior. However, in actual practice their measured mechanical properties are parallel to those of the open cell metallic foams having the same relative density, that is the strength contribution from the cell faces are low since they buckle/rupture easily.[165,166]

Concerning brittle cellular solids, Brezny and Green[167] proposed that the relative density is the chief factor for defining the mechanical properties, which was later supported by other studies.[168] It is also known that brittle porous structures like C&Gs are subjected to a size effect because of greater probability of finding critical defects (microcracks). Accordingly, closed-cell solid foams with enhanced mechanical properties might be obtained (compared to that of the open cell ones at the same relative density) if the skeletal defects can be eliminated. This simply means to move toward the GA model (ie, upper-bound) assuming that the strut modulus of the rupture is constant which in reality varies following Weibull distribution, implying also that with the same relative density, the crushing strength decreases with the increase in pore size.[161]

In accordance with above, the study[169] suggested higher defect probability in the thicker struts for macrocellular ceramics. At the same relative density, microcellular ceramics showed higher crushing strength than those of the macrocellular ones. The effect of cell size on compressive strength for these ceramics can be seen in Figure 15A.[169–171] Similarly, exceptional high-mechanical strength values were claimed for closed porosity microcellular SiOC monoliths showing ~100 MPa compressive strength at $\phi_T = 70\%$. Such unprecedentedly high strength was attributed both to the small pore size (<30 μm) and to the lack of matrix defects.[14] In Figure 15B the data extracted from the published works for pore size versus compressive strength are plotted. As seen the growth trend of strength is actually an exponential with the decrease in pore size especially for the ones below 50 μm.

The theoretical expressions given above assumes the fracture behavior of the cells as bending dominated which is indeed the deformation behavior of the most open and closed porosity components. Ashby, F. M.,[164] and Deshpande et al[165] in accordance with the Maxwell's stability criterion[172] demonstrated that, see Figure 16A,B, the lattice connectivity (ie, average number of trusses/beams at a node/joint) below a threshold imposes bending-dominated behavior while above the limit, the deformation is predominantly stretch-dominated. Bending-dominated structure is weaker but still a better energy absorber under compression compared to that of stretch-dominated structure constituted by triangles (2D) or tetrahedrons (see Figure 16C,D) for a 3D stretch-dominated unit cell together with microtruss structure) analogues to several civil engineering load-bearing structures (eg, bridges) which are strong and stiff for a given mass.[162]

It is no surprise that at the same relative density, the initial collapse strength and the elastic modulus of stretching dominated cellular materials are higher than those of bending-dominating ones.[174] The former one possesses tension-compression deformation mode (hard), while the latter bends (soft). As a consequence, strut-stretching mechanical response should be considered for applications where higher stiffness and strength

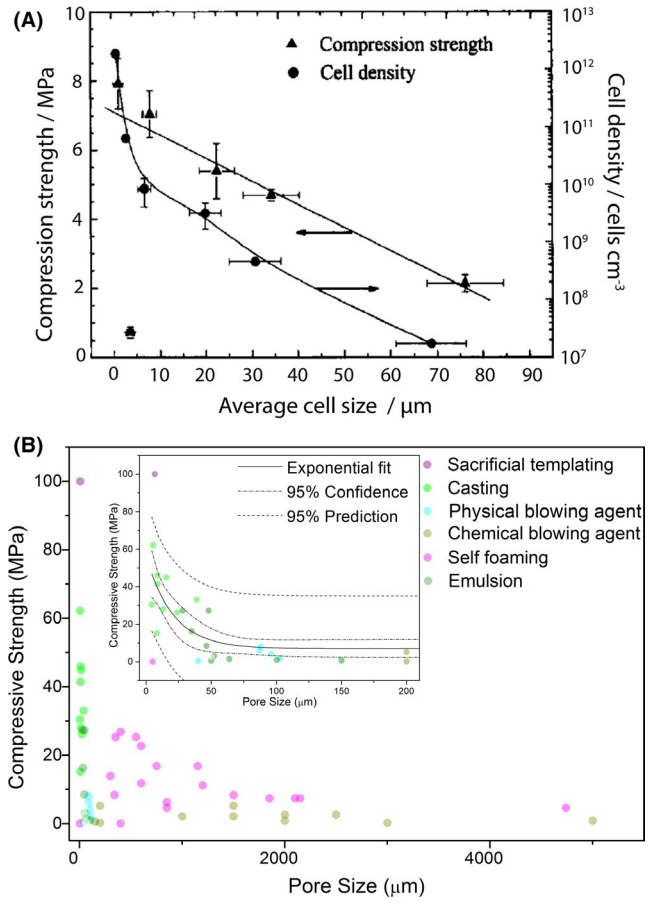

FIGURE 15 (A) For open-porosity SiOC microcellular foams, compression strength data are given as a function of the average cell size (Reproduced from[169] with permission John Wiley and Sons, Copyright 2004), and (B) pore size (μm) vs compressive strength (MPa) data collected from published papers (no data were found for high-temperature bonding of hollow structures), the inset demonstrates the detail of the plot below 250 μm pore size with exponential fit and corresponding 95% confidence and prediction interval

at low weight is sought, for example lightweight structural applications. However, these structures have post-yield softening responses due to strut buckling or crushing (brittle materials), making them less suitable for steady stress-strain response requiring applications, such as energy absorbers, see comprehensive chapter for details.[175] In general, stress-strain response of a porous solid material under compression test has three distinct regions, namely linear elastic, a fingerprint deformation mode which is constant plateau or a post-yield softening, and densification due to eventual contact of the cell struts/edges generating a pure geometric effect so that additional bending/buckling/crushing is not anymore possible.

Most of the man-made porous solids (both open and close cell) have bending-dominated, nontriangular strut/truss structures. For the closed-cell structures, cell faces do not contribute much to the strength and the cell edges carry the load in major part, analogous to low strut-connectivity open cell foams.[12] By increasing the strut connectivity (Maxwell's criterion)[172] stretch-dominated microtruss/strut architectures, typified by triangulated lattices (tetrahedrons), could as well be designed.[173] Without increasing the strut connectivity, a variant adjustment can be adopted from the nature where hierarchically structured materials manifesting multiple mechanical responses are seen, that is not only bending or stretching modes. In real practice such structures, especially in microscale, with accurate and detailed geometries are extremely difficult to manufacture by traditional or conventional processes, and currently only manifested by AM.

Impact absorbing is another key mechanical property for the end-use of many commercial products. Porous components find applications as energy absorbers for different applications such as vibration damping/packaging layers for transport industries, impact absorbers for space, automobile, sport, etc[12,161,180] Impact absorbing materials are designed to dissipate the shock kinetic energy by different mechanisms for example

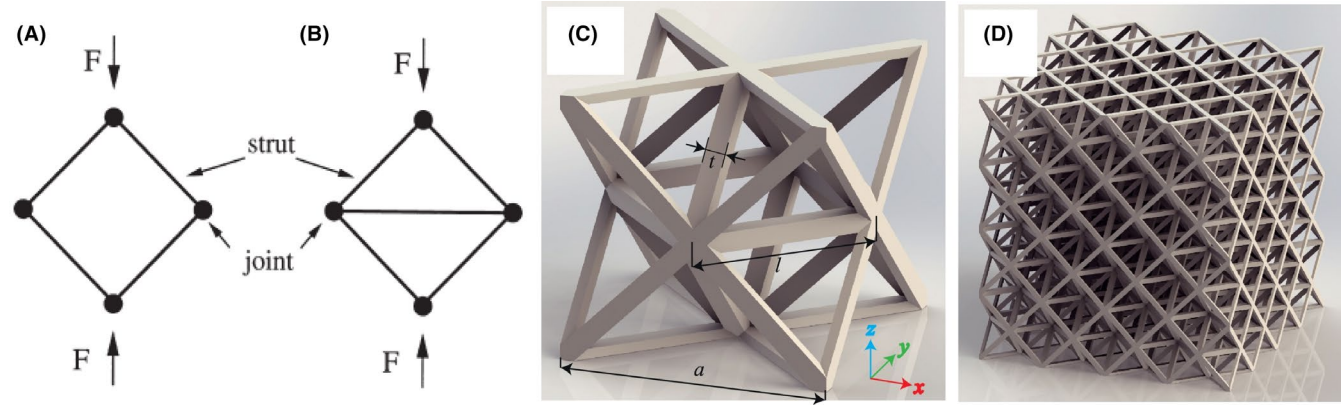

FIGURE 16 A and B, Assuming the joints in both frames are fixed, on loading the first (A) struts bend due to bending moments on the nodes, that is a bending-dominated structure. Although struts bend similarly in the frames given in (B), the collapse load is dictated mainly by the axial strength of the struts, that is stretching-dominated structure (Reproduced from[165] with permission Elsevier, Copyright 2001), (C and D) examples of a stretch-dominated 3D unit cell and a microtruss structure (Reproduced from[173] with permission Elsevier, Copyright 2017)

PANEL III: Additive manufacturing

Additive manufacturing (AM), so called 3D printing, creates unprecedented opportunities to form porous components with desired cell architecture (quantity, shape, and size). AM is basically a method to shape a porous ceramic which is produced by any of the methods already described above. It can be used to produce intricate geometries and it is possible to mimic the hierarchical organization of the natural materials like bamboo, wood, etc (ie, architecture of the load-bearing units at different length scales) that are virtually impossible to manufacture with other techniques. This is because the technique enables accurate design and engineer the truss/filament members (current resolution boundaries will certainly be resolved in the near future), so that it is possible to obtain not only the microtruss structural formations but even nanotruss-architectured materials having tunable mechanical responses.[176]

Concurrent usage of AM with other methods (eg, emulsified wet foam 3D printing) provides design freedom so that not just sophisticated shapes (microarchitected truss structures) and precise control of the pore character becomes possible but also less defected structures and consequently enhanced strength is attainable. However, currently there are still problems such as low density and resolution, poor surface finish, flaws, and most importantly very high cost (of one-pot printing devices) for small lot manufacturing.

Wet foams synthesized by Muth et al[177] were used to obtain predefined, bio-inspired hierarchical architectures with mixed mode mechanical responses; in Figure 17A-C, anode with multiple strut connectivity and inner microstructure is given. The manufactured components had bending-dominated hexagonal or stretching-dominated triangular trusses constituted by closed porosity (or nearly dense) imposing additional bending-dominated response by altering the processing parameters (ink composition, geometry, dry and sintering). In such a way, it was possible to control mechanical responses being bending, stretching, bending-bending, or stretching-bending, and so the elastic modulus of the samples was able to be altered from around 1 GPa (hexagonal struts with closed porosity) to 27 GPa (triangular nearly dense struts).

Another example was demonstrated by Minas et al[178] via the preparation of emulsions (α-Al_2O_3 with 200 nm particle size), followed by direct ink writing (DIW) of synthesized wet foams as cubic lattices. The heat-treatment process (1600˚C/2 h) resulted in the lattices having total porosity above 90%, constituted by filaments (trusses) which can be designed as dense, open or closed porosity by process control. Very recently, fly ash hollow spheres were used to obtain closed porosity (reaching around 90%) mullite ceramics by selective laser sintering (SLS) as well.[179]

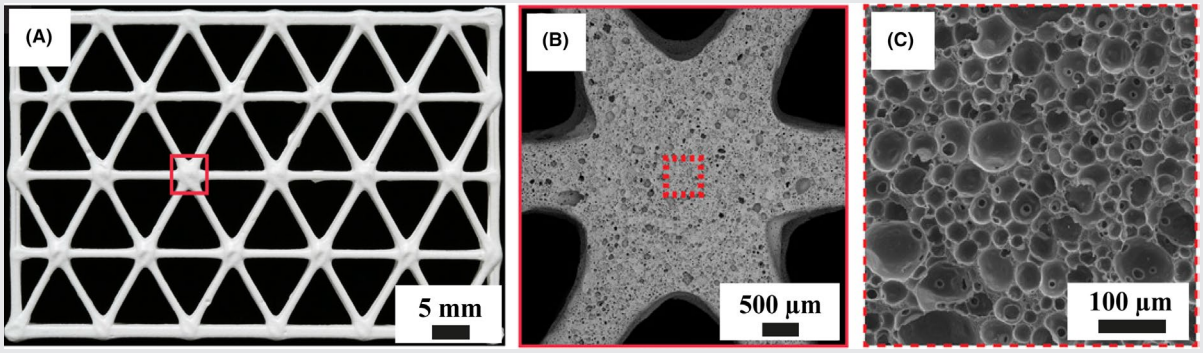

FIGURE 17 (A) Printed and sintered component with triangular cells, and (B) the close magnification image of a node, and (C) the resulting SEM image showing the closed porosity microstructure of the node (Reproduced with permission from[177])

viscoelastic or plastic deformations (the material is used only once). However, while closed porosity structures (generally cellular polymers) used in abovementioned applications, there are no published data on the impact absorption capacity for the closed porosity C&Gs yet. Another potential utilization can be found in biomaterials field for example for hard tissue replacement/implant applications. As known, hierarchical architecture of the human bone provides superior strength and the stiffness of the synthetic bone material can be altered by close porosity.[181]

3.2 | Thermal behavior

Thermal insulation is one of the key application areas that utilize cellular ceramics, a better insulation means less energy consumption and reduced amount of CO_2 release for both industrial processes and buildings. For other applications, it means safety; as known, for example, the space shuttle Columbia sadly disintegrated upon reentering Earth's atmosphere and one of the reasons for such tragic event was found to be the slumping of the thermal protection system (TPS) tiles.[182] When thermal properties are of importance, thermal conductivity (λ), thermal shock resistance (crucially important for high-temperature utilization as refractory, solar receiver, heat exchanger, porous burner, and molten metal filters, etc), and heat capacity (C) should be evaluated.

Porous materials can be assumed as two phase components created by a matrix phase and a "space holder/filler" phase being usually a gas. For such components not only the thermal properties of a solid matrix but also heat transfer modes of the pore filling phase should be taken into account. Gases can transfer heat through conduction, convection, and radiation. However, natural convection necessitates large bulk flow of the gas, that is only when the Grashof number (Gr) is $\geq$ 1000 which accounts for the pore size about 10 mm.[12,161] This size is way larger than the pore dimensions usually seen in porous components, especially for the closed porosity components. Due to that, the natural convection contribution to overall thermal conductivity is assumed negligible for closed porosity C&Gs.

Concerning above, the thermal conductivity is governed by the combination of (a) conduction (ie, phonon conductivity) through the solid matrix (struts and cell faces/walls), and through the space filling material (gas, generally air), (b) radiation (ie, photon conductivity; usually significant at elevated temperatures). Heat transfer via electrons is insignificant for C&Gs since the charge is localized, unlike metallic materials having free electrons. Therefore, the overall quantitative insulation performance of porous brittle solids is analyzed by effective thermal conductivity (λ_{eff}) as given in Equation (6); where $\lambda_{cond.(solid)}$ is thermal conductivity of the solid skeleton, $\lambda_{cond.(gas)}$ is the thermal conductivity of the gas which is affected by both temperature (T) and gas pressure (P_g), and $\lambda_{rad.}$ is the radiative conductivity.[183]

$$\lambda_{eff.(T,\,Pg)} = \lambda_{cond.(solid\ (T))} + \lambda_{cond\ (gas\ (T,\,Pg))} + \lambda_{rad.(T)}. \quad (6)$$

Gases have poor thermal conductivities compared with that of any solid material (eg, free air at 20°C has 0.0257 W/m.K. and Al_2O_3 has around 25 W/m.K.).[12] If gas bubbles can be homogenous trapped in the solid matrix, the resulting two-phase material will have lower effective thermal conductivity than that of the solid phase alone. This is particularly important when the gas bubbles are distributed in the small-sized isolated pockets which diminishes convection (no bulk gas flow) and restricts radiation (via absorption, scattering, reflection on the cell surfaces), making the closed porosity materials with the lowest effective conductivity in the nonvacuum conditions.[184]

Amorphous solids have lower thermal conductivities than that of the corresponding crystalline solids due to enhanced phonon scattering. With the increase in temperature these two solids behave differently concerning the solid thermal conductivity;[185] however, still the outcome is insignificant above RT since the radiative conductivity becomes dominant and it is believed to be proportional with the cube of temperature (T^3).[183,186,187] This is particularly important for amorphous materials, transparent crystals and porous structures.[188] Considering all above, closed porosity amorphous materials can be designed so as to reduce effective thermal conductivity further. In this regard, closed porosity (~80%) silica components were produced by hollow silica spheres. When the generation of cristobalite was hindered, a better insulation performance was observed. The process resulted in the samples having λ_{eff} = 0.102-0.218 W/m.K. at RT. As expected, the increase in the closed porosity caused a decrease in the effective thermal conductivity.[40]

Similarly, closed porosity (ϕ_T = 56%-79%) borosilicate glass components were formed by hollow glass microspheres, the samples with 25% solid loading demonstrated low-effective thermal conductivity (0.07 W/m.K. at RT), and proposed to find application as thermal insulators for aerospace industry, undersea pipeline, and submarines.[41]

Oxides are useful materials especially for high-temperature shielding applications since they have good oxygenation resistance and durability. Among those, zirconia is one of the best candidates due to its very low-thermal conductivity (2.0 W/m.K., dense). Aimed for the refractory applications, closed porosity (ϕ_T reaching 98%) zirconia foams with low-thermal conductivity values (0.027 W/m.K. at RT) were able to be produced.[150] In another study, granite scraps and clay tailings were used to form closed porosity ($\phi_T \sim$ 83%) mixed oxides having reasonably low-effective thermal conductivity (0.051 W/m.K.), intended for building insulations.[81] Porous anorthite/gehlenite ceramics ($\phi_T <$ 60%) were fabricated from clays and paper processing residues. Such monolithic bodies with λ = 0.42-0.83 W/m.K. were aimed to be used at high temperatures like 1200°C as backup refractory for kilns/furnaces.[19]

Zirconium carbide is a transition metal carbide in the family of ultra-high temperature ceramics (UHTC, with $T_{melting}$> 3200°C, good hardness and thermo-mechanical properties), and often associated with wide range of high-temperature applications such as hypersonic vehicles (aerospace) or in nuclear industry.[189] Closed porosity (ϕ_T = 85%, cell size of ~ 40 μm) ZrC foam with effective thermal conductivity of 0.94 W/m.K. (at 50°C) and of 1.36 W/m.K. (at 300°C) was

made via two step synthesis; formation of preceramic foam from zirconia sol and phenolic resin. The authors demonstrated that the overall effective thermal conduction increases (up to 300°C limited by the apparatus) with increasing temperature, note that the plot in Figure 18A does not resemble proper T^3 behavior.[53] Similar observations were done by other studies; Bourret et al[63] showed that the radiation contribution was lower than 10% at RT (where conduction was the predominant heat-transfer mechanism), but increased to more than 50% at 500°C, see Figure 18B for the effect of temperature on thermal conductivity with and without radiation contribution.[63] This is due to the fact that radiative heat transfer within the pores increases with the cube of the temperature.[161] It should be recalled that the properties of the entrapped gas in the pores might have an influence on the final insulation characteristics of the formed component, that is the thermal conductivity for CO_2 is 0.016 W/m.K. and for N_2 is 0.025 W/m.K. at RT.[85,190]

Thermal shock resistance (R_{TS}) is the ability to withstand the stresses caused because of sudden temperature changes, instead thermal (stress) fatigue is a failure due to cyclic thermal stresses/strains caused by temperature fluctuations. While the latter has not been investigated thoroughly for closed porosity C&Gs,[191] the R_{TS} of brittle materials has been well-documented,[192] and known to be affected by the elastic modulus, thermal conductivity, thermal expansion coefficient, strength, and the Poisson's ratio.[193] Although the details can be found in related literature,[11,161,194] the R_{TS} increases by reduction in the foam density because the struts can accommodate the generated strain (thermal) by bending.[161] Besides, it was shown that the introduction of small amount of porosity may enhance the R_{TS} since the thermal stresses can be relaxed by the presence of pores, arresting the crack propagation.[195,196] Inspired from this idea, 3YSZ and 3YSZ/zircon ($ZrSiO_4$) ceramics having relatively low amount of porosity (<30%) were manufactured with the goal of producing permanent molten metal (brass) casting molds.[197]

3.3 | Electrical and other properties

The most commonly investigated electrical property for porous ceramics so far is the dielectric constant.[28,151] Yamamoto et al[214] described that the dielectric constant of the glass-ceramic substrates, intended to be used in integrated circuit packaging, could be decreased by deliberately formed and homogenously distributed closed porosity. This is because according to the general Lichterecker mixing rule;[215] introduction of the lower polarizable secondary phase decreases the dielectric constant of the primary phase which could be done either by addition of "gas" (air or others with values not far from to that of the vacuum; $\varepsilon = 1$) into the matrix phase as an isolated secondary phase, that is creating a porosity or by the addition of light elemental oxides such as Li_2O or B_2O_3.[216] Following the idea, alumina/glass samples with well-dispersed closed porosity (33%) and dielectric constants as low as 5.1 were obtained.[28] In another study,[151] BST closed porosity ceramics ($\phi_T < 95\%$) were formed by particle-stabilized foaming. The samples exhibited low-dielectric constant (47-150) and dielectric loss values below 0.0025. The introduction of porosity in BST ceramics effectively decreased the dielectric constant without harming the tunability which could be used as acoustic impedance adjustment and over-current protectors.[217]

Ideally for wave-transparent materials, it is necessary to have a low-dielectric constant and loss tangent value to be used as radomes or antenna windows.[218] These antenna protection systems should be made of a material having adequate strength together with transparency to the signals received and transmitted by the antenna (better to have a broadband capability). Radomes used in aircrafts or missiles traveling at supersonic/hypersonic speeds may expose to temperatures above 1400°C. Thus, such material not only should be wave transparent but also be of high temperature, thermal fatigue, and thermal shock resistance.[219] Closed porosity BN ceramics demonstrated to have characteristics that make them suitable

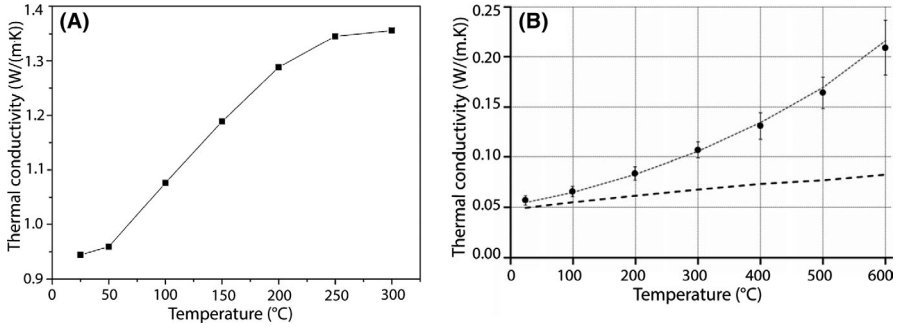

FIGURE 18 (A) For closed-cell ZrC ceramic foams, the effect of temperature on the effective thermal conductivity (Reproduced from[53] with permission Elsevier, Copyright 2014) and (B) effective thermal conductivity of a closed-cell ceramic foam made by using kaolin clay as a function of temperature, in the data the dashed lines demonstrate the thermal conductivity without the radiation contribution (Reproduced from[63] with permission John Wiley and Sons, Copyright 2014)

PANEL IV: Foamed concrete and syntactic foams

Among the various industrial application areas of closed porosity C&Gs, two of the most common ones in which decent mechanical properties at lightweight rationalized are cellular concretes and *syntactic foams.* The details related with these specific materials have been left out and interested reader is referred to published literature.[83,198–201]

In the building industry, the most commonly used cellular concretes are aerated concrete (AC) and foamed concrete (FC). For the production of AC, cement mortar is prepared from the mixture of cement, gypsum, lime, sand, and sometimes with fly ash or other additives and water. The blend is then mixed with a small amount of CBA (called as aerating agent and the most commonly used ones are hydrogen peroxide/bleaching, calcium carbide and aluminum.[202]) which reacts with the paste and produces gas.[83] In the next stage, if autoclave treatment is followed, the structure strengthens by hydrothermal reactions (via the formation of calcium silicate hydrates, eg, tobermorite, xonotlite).[21,203]

Instead FC is a partially closed porosity material formed with the help of foaming agents such as detergents, glue resins, etc (ie, no chemical reaction with ingredients during the curing process). The foamed concrete term somehow misleads since there is no similar aggregate utilization as in case for concrete production and the material is basically a cement mortar. FC has few ingredients in the base mixture: cement, water, and foaming agent to generate gas bubbles which can be stabilized with the additives to solidify as isolated pores after curing.[204] Foaming can be conducted either via preformed method in which foaming agent is mixed with water and aerated prior to addition into the blend, or mix-foaming in which foaming agent is added directly in to the blend. While the bulk density of the FC components ranges in between 0.5 and 2.0 g/cm^3, the ratio of the open/closed porosity was shown to be altered by processing conditions

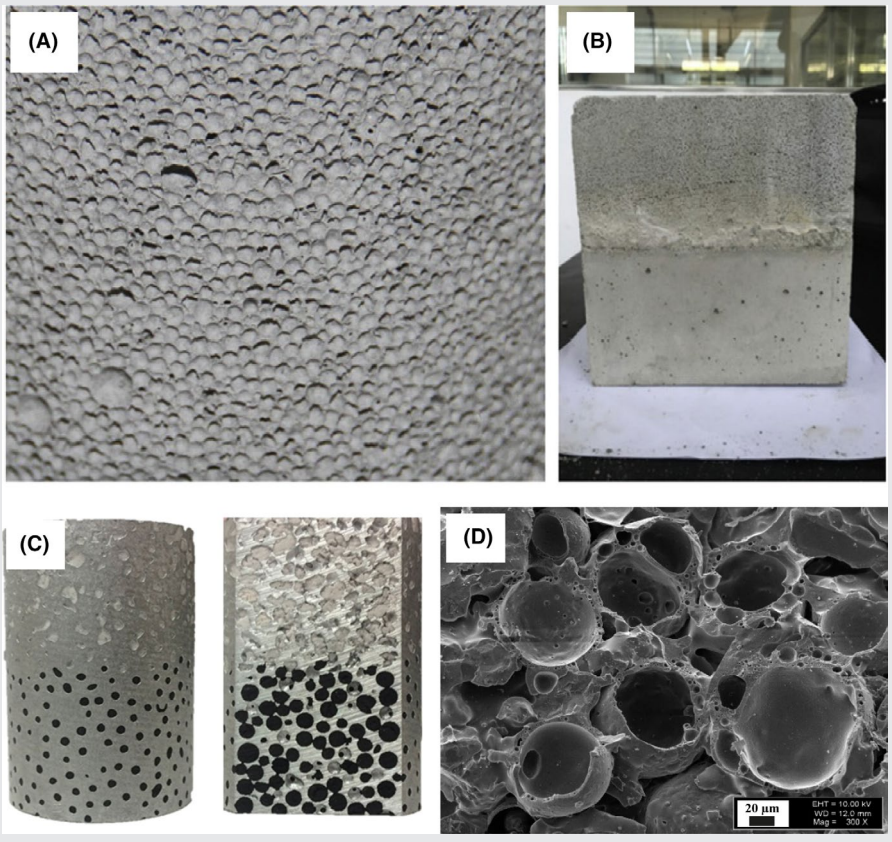

FIGURE 19 Images of foamed concrete samples made from water, cement, and foaming agent; (A) cellular structure showing closed-cells and (B) cubic-shaped components for which the upper half was prepared by using foamed concrete and the bottom half was only concrete for specific tests (Reproduced from[212] with permission Chinese Academy of Sciences), (C) Image of truncated functionally graded metal syntactic foam (Reproduced from[213] with permission Elsevier, Copyright 2019) and (D) SEM microstructure of clay-cenosphere made ceramic matrix syntactic foam showing hollow microspheres (Reproduced with permission from[31])

such as water/cement/foaming agent ratio. The pore size of the final material can be controlled by the cement paste viscosity and foaming agent.[205] FC is a decent construction material since it has high-specific strength, seismic and freeze/thaw performance emerging due to closed porosity, see Figure 19A,B for representative examples.[83,201,206] FCs with various bulk densities were tested concerning their mechanical properties at higher temperatures.[207] The results demonstrated that as soon as the temperature exceeds 90°C the loss of water induces microcracking. While the initial reduction in compressive strength was about 6%, above 200°C significant reduction occurred and at 400°C only 75% of the initial value remained regardless of initial bulk density.

Syntactic foams have been used in automobile, infrastructure, marine (subsea buoyancy), and aerospace industry for years. They are basically composites made by embedding micron-sized hollow spheres inside a matrix (metal, ceramic or polymer), see Figure 19C,D. Any hollow structure (cenospheres, glass microspheres, carbon, etc) can be used with any matrix material to tailor the final properties.[31,166] Ceramic syntactic foams were usually formed either by casting,[38,40,41,45] by semi-dry techniques,[31] or by PP infiltration[208–210] using hollow microspheres. For those, raw materials used to generate the matrix (skeleton) and the porosity have different chemistry, consequently it was difficult to control the final ceramic composition and generally the multiphase materials were obtained. Alternatively, by using hollow spheres as the only raw material (ie, both matrix and pore former being the same material) closed porosity phase-pure C&Gs can be formed by high-temperature bonding. Otherwise, initially formed microbeads can be infiltrated by the same chemical composition derivable PP.[4,211]

as radome since RT dielectric constant and loss tangent values were as low as 1.25 and 0.0031, respectively. Increasing the test temperatures up to 1300°C caused a slight rise in the values but they were still acceptable to be high-temperature wave-transparent material.[121]

In a basic definition, sound absorption means dissemination of the incident sound wave energy in the material with no reflection or transmission. While for passive insulation mediums such energy absorption can proceed by several different mechanisms (viscous losses, thermal-elastic damping, Helmholtz resonance, sharp edge vortex shedding, direct mechanical damping, etc)[220], for stiff and porous absorbers such as C&G foams, sound energy depletion occurs in the interconnected pores principally by viscous friction, transforming it to thermal energy and leading to wave attenuation.

While in some published works, closed porosity C&Gs are advised to be used for sound absorption. It is clear that purely closed porosity C&Gs have low-sound absorption capability since they cannot provide air permeability, besides their high stiffness which does not allow absorption via vibration.[220–222] Some applications such as acoustic liners inside combustion chambers (high temperature stability and absorption), noise barriers in road tunnels (high strength and absorption), pick up impedance for the ultrasound source have already been proposed in the literature for cellular ceramics;[12,221–224] however, to the best of our knowledge, there are no studies reporting the sound absorption capacity of the closed porosity ceramics in a comparative manner with the ones having complete open-porosity yet. Mixed porosity (ϕ_C = 34% of ϕ_T = 75%) TiO_2-based components designed as engine front silencer, but the closed porosity was only for strength alteration and inactive for sound attenuation.[225] It should be noted that some modifications like perforation, surface removal, deliberate pore surface fracturing, etc could be done to enhance the sound absorption properties for closed porosity ceramic materials especially for high-temperature applications. This was already conducted on the closed-cell metallic materials and significant enhancement was observed.[226]

4 | SUMMARY AND FUTURE PERSPECTIVES

The current status of the processing techniques, the properties, and the application areas for the close porosity C&Gs are discussed. The production techniques are fundamentally categorized as sacrificial templating, high-temperature bonding of hollow structures, casting, direct foaming, and finally emulsion making. Specific issues are discussed in four different panels, namely (a) solid-state foaming (thermodynamic instability) technique which has long been used to produce porous metallic and polymeric materials, (b) foam glass and glass ceramics, (c) foamed concrete and syntactic foams, and (d) additive manufacturing (AM), which can be, in principle, used in combination with any of the previously mentioned processing techniques, and can be successfully implemented to process the porous components with desired cell architecture (quantity, shape, and size). It is possible to construct stable lightweight closed porosity C&G structures and geometries by AM that cannot be produced using traditional manufacturing processes. Concerning the shaping, it is worth to state that in general porous ceramics are quite tough especially those with high porosity, and therefore, they can be easily machined into the desired final shapes.

From a theoretical point of view, for the same chemistry/porosity level the crushing strength of a closed porosity C&G increases when: (a) the matrix (struts and pore walls) is dense, (b) the structure is composed of pores being as small as possible (this implies also reduced defect size), and usually (c) there is regularly distributed (homogeneous) porosity. Generally, due to the fact the struts/necks of high-temperature fused materials have reduced amount of skeletal defects, it is possible to expect higher mechanical performance compared to those of other techniques. Unfortunately, for such method, limited amount of chemistries are available to be used as hollow structures. Besides, production of components with pore sizes below micron level remains a challenge, and therefore apparently emulsion technique seems to be the most suitable technique to obtain materials with the best mechanical performance. A similar trend can be identified for thermal conductivity. Generally, to decrease the thermal conductivity the ideal microstructure should be: (a) highly porous; (b) constituted by porosity with as small as possible pore size; (c) having an amorphous matrix, and (d) for insulation at high temperature, the glassy material should be substituted with high-refractory ceramics (eg, alumina).

The preparation of novel compositions and the development of innovative fabrication techniques should become the object of future research that will permit a further extension of the features in terms of defect-free matrices, tunable pore size, shape, and distribution. Besides, systematic studies should be carried out to address the effect of pore characteristics (especially for pore size and volume, in a comparative way with open porous samples having similar chemical composition) on the mechanical and other properties stated above. In this way, closed porosity C&Gs with wide variety of properties can be obtained for their potential use in the applications as lightweight building industry (eg, water-proof floors/roofs with less material consumption, novel deep water buoyancy mediums or cable buoys), thermal insulation systems for household and industrial appliances (saving energy and reducing greenhouse gas emissions), thermal protection system for high-speed vehicles such as space shuttles (securing the shuttle integrity and decreasing the overall construction costs due to re-usability), low-dielectric insulators for micro/nano-electronic packaging (reducing power consumption and cross talk, thus improving the chip performance which is critically important especially for portable devices) or even drug-delivery systems in which the cargo molecules can be loaded in the closed cells and the release can be triggered by the dissolution of the matrix (eg, a calcium phosphate or bioactive glass phase) in a controllable time frame.

ACKNOWLEDGMENTS

The authors thank Hazal Dengiz (Visual communication design, TOBB University of Economics and Technology), Evrim Yakut Evecen (Izmir Institute of Technology), Gun Deniz Akkoc (Department of Chemistry, Izmir Institute of Technology), and other group members: Levent Karacasulu, Ezgi Ogur, Ecem Ozmen, Oyku Icin, and Cerem Piskin (Department of Materials Science and Engineering, Izmir Institute of Technology) for their helps during the preparation of schematics and literature survey.

ORCID

Cekdar Vakifahmetoglu https://orcid.org/0000-0003-1222-4362
Tugce Semerci https://orcid.org/0000-0001-7226-5559
Gian Domenico Soraru https://orcid.org/0000-0002-0453-3379

REFERENCES

1. Vakifahmetoglu C, Zeydanli D, Colombo P. Porous polymer derived ceramics. Mater Sci Eng R. 2016;106:1–30.
2. Schüth F, Sing KSW, Weitkamp J. Handbook of porous solids. Weinheim: Wiley-VCH, 2002.
3. IUPAC. Compendium of chemical terminology, 2nd ed. (the "Gold Book"). Compiled by A.D. McNaught and A. Wilkinson. Oxford: Blackwell Scientific Publications, 1997. Online version: doi: https://doi.org/10.1351/goldbook (2019-) created by S. J. Chalk.
4. Vakifahmetoglu C, Zeydanli D, de Mello Innocentini MD, dos Santos RF, Lasso PRO, Soraru GD. Gradient-hierarchic-aligned porosity SiOC ceramics. Sci Rep. 2017;7:41049.
5. Colombo P. Conventional and novel processing methods for cellular ceramics. Philos Trans Royal Soc A. 2006;364:109–24.
6. Studart AR, Gonzenbach UT, Tervoort E, Gauckler LJ. Processing routes to macroporous ceramics: a review. J Am Ceram Soc. 2006;89:1771–89.
7. Colombo P, Vakifahmetoglu C, Costacurta S. Fabrication of ceramic components with hierarchical porosity. J Mater Sci. 2010;45:5425–55.
8. Guzman IY. Certain principles of formation of porous ceramic structures. Properties and applications (a review). Glass Ceram. 2003;60:280–3.
9. Luyten J, Mullens S, Thijs I. Designing with pores-synthesis and applications. KONA Powder Part J. 2010;28:131–42.
10. Ohji T, Fukushima M. Macro-porous ceramics: processing and properties. Int Mater Rev. 2012;57:115–31.
11. Rice RW. Porosity of ceramics: properties and applications. New York: CRC Press, 1998.
12. Scheffler M, Colombo P. eds. Cellular ceramics: structure, manufacturing, properties and applications. Chichester: John Wiley & Sons, 2006.
13. Ishizaki K, Komarneni S, Nanko M. Porous materials: process technology and applications. Dordrecht: Springer Science+Business Media BV, 1998.
14. Kim Y-W, Jin Y-J, Chun Y-S, Song I-H, Kim H-D. A simple pressing route to closed-cell microcellular ceramics. Scr Mater. 2005;53:921–5.
15. Kim S-H, Kim Y-W, Park C. Effect of inert filler addition on pore size and porosity of closed-cell silicon oxycarbide foams. J Mater Sci. 2004;39:3513–5.
16. Kim Y-W, Kim S-H, Kim H-D, Park CB. Processing of closed-cell silicon oxycarbide foams from a preceramic polymer. J Mater Sci. 2004;39:5647–52.

17. Kim Y-W, Wang C, Park CB. Processing of porous silicon oxycarbide ceramics from extruded blends of polysiloxane and polymer microbead. J Ceram Soc Jpn. 2007;115:419–24.
18. Thijs I, Luyten J, Mullens S. Producing ceramic foams with hollow spheres. J Am Ceram Soc. 2004;87:170–2.
19. Sutcu M, Akkurt S. Utilization of recycled paper processing residues and clay of different sources for the production of porous anorthite ceramics. J Eur Ceram Soc. 2010;30:1785–93.
20. Sutcu M, Akkurt S. The use of recycled paper processing residues in making porous brick with reduced thermal conductivity. Ceram Int. 2009;35:2625–31.
21. Vakifahmetoglu C. Zeolite decorated highly porous acicular calcium silicate ceramics. Ceram Int. 2014;40:11925–32.
22. Tulliani JM, Lombardi M, Palmero P, Fornabaio M, Gibson LJ. Development and mechanical characterization of novel ceramic foams fabricated by gel-casting. J Eur Ceram Soc. 2013;33:1567–76.
23. Green DJ. Fabrication and mechanical properties of lightweight ceramics produced by sintering of hollow spheres. J Am Ceram Soc. 1985;68:403–9.
24. Verweij H, De With G, Veeneman D. Hollow glass microsphere composites: preparation and properties. J Mater Sci. 1985;20:1069–78.
25. Boccaccini AR. Fabrication, microstructural characterisation and mechanical properties of glass compacts containing controlled porosity of spheroidal shape. J Porous Mat. 1999;6:369–79.
26. Geng H, Hu X, Zhou J, Xu X, Wang M, Guo A, et al. Fabrication and compressive properties of closed-cell alumina ceramics by binding hollow alumina spheres with high-temperature binder. Ceram Int. 2016;42:16071–6.
27. Zhao F, Ge T, Gao J, Chen L, Liu X. Transient liquid phase diffusion process for porous mullite ceramics with excellent mechanical properties. Ceram Int. 2018;44:19123–30.
28. Wu S, Jonghe LD. Alumina-coated hollow glass spheres/alumina composites. J Mater Sci. 1997;32:6075–84.
29. Omatete OO, Janney MA, Nunn SD. Gelcasting: from laboratory development toward industrial production. J Eur Ceram Soc. 1997;17:407–13.
30. Ortega FS, Valenzuela FAO, Scuracchio CH, Pandolfelli VC. Alternative gelling agents for the gelcasting of ceramic foams. J Eur Ceram Soc. 2003;23:75–80.
31. Rugele K, Lehmhus D, Hussainova I, Peculevica J, Lisnanskis M, Shishkin A. Effect of fly-ash cenospheres on properties of clay-ceramic syntactic foams. Materials. 2017;10:828.
32. Rawlings R, Wu J, Boccaccini A. Glass-ceramics: Their production from wastes-a review. J Mater Sci. 2006;41:733–61.
33. Hirajima T, Oosako Y, Nonaka M, Petrus H, Sasaki K, Ando T. Recovery of hollow and spherical particles from coal fly ash by wet separation process. J MMIJ. 2008;124:878–84.
34. De Belie N, Soutsos M, Gruyaert E. Properties of fresh and hardened concrete containing supplementary cementitious materials. Cham, Switzerland: Springer, 2018.
35. Dwivedi A, Jain MK. Fly ash waste management and overview: a review. Recent Res Sci Technol. 2014;6:30–5.
36. Guo R, Rohatgi P. Chemical reactions between aluminum and fly ash during synthesis and reheating of Al-fly ash composite. Metall Mater Trans B. 1998;29:519–25.
37. McBride SP, Shukla A, Bose A. Processing and characterization of a lightweight concrete using cenospheres. J Mater Sci. 2002;37:4217–25.
38. Wang C, Liu J, Du H, Guo A. Effect of fly ash cenospheres on the microstructure and properties of silica-based composites. Ceram Int. 2012;38:4395–400.
39. Huo W, Zhang X, Chen Y, Lu Y, Liu J, Yan S, et al. Novel mullite ceramic foams with high porosity and strength using only fly ash hollow spheres as raw material. J Eur Ceram Soc. 2018;38:2035–42.
40. Sun Z, Lu C, Fan J, Yuan F. Porous silica ceramics with closed-cell structure prepared by inactive hollow spheres for heat insulation. J Alloys Compd. 2016;662:157–64.
41. Ren S, Guo A, Dong X, Tao X, Xu X, Zhang J, et al. Preparation and characteristic of a temperature resistance buoyancy material through a gelcasting process. Chem Eng J. 2016;288:59–69.
42. Fey T, Zierath B, Greil P, Potoczek M. Microstructural, mechanical and thermal characterization of alumina gel-cast foams manufactured with the use of agarose as gelling agent. J Porous Mat. 2015;22:1305–12.
43. Luyten J, Mullens S, Cooymans J, De Wilde AM, Thijs I, Kemps R. Different methods to synthesize ceramic foams. J Eur Ceram Soc. 2009;29:829–32.
44. Dhara S, Bhargava P. Influence of slurry characteristics on porosity and mechanical properties of alumina foams. Int J Appl Ceram Tec. 2006;3:382–92.
45. Shao Y, Jia D, Zhou Y, Liu B. Novel method for fabrication of silicon nitride/silicon oxynitride composite ceramic foams using fly ash cenosphere as a pore-forming agent. J Am Ceram Soc. 2008;91:3781–5.
46. Chen XX, Du JH, Gan GY, Yan JK, Yi JH. Effect of solid content on performance of porous alumina ceramic by gel-foaming. Adv Mater Res. 2012;476–478:1007–10.
47. Colonetti VC, Sanches MF, de Souza VC, Fernandes CP, Hotza D, Quadri MGN. Cellular ceramics obtained by a combination of direct foaming of soybean oil emulsified alumina suspensions with gel consolidation using gelatin. Ceram Int. 2018;44:2436–45.
48. Faber KT, Shanti NO.Gelcasting of ceramic bodies. In: Bansal NP, Boccaccini AR, editors. Chapter 6 in ceramics and composites processing methods. Hoboken, NJ: John Wiley & Sons; 2012.
49. Chen Q-Z, Thouas GA. Fabrication and characterization of sol–gel derived 45S5 Bioglass®–ceramic scaffolds. Acta Biomater. 2011;7:3616–26.
50. Li F, Liang M, Ma X-F, Huang X, Zhang G-J. Preparation and characterization of stoichiometric zirconium carbide foams by direct foaming of zirconia sols. J Porous Mat. 2015;22:493–500.
51. Fukushima M, Ohji T, Hyuga H, Matsunaga C, Yoshizawa Y-I. Effect of gelatin gel strength on microstructures and mechanical properties of cellular ceramics created by gelation freezing route. J Mater Res. 2017;32:3286–3293. 03/28.
52. Heck RLIII, Peascoe WJ. Blowing agents. In: Mark HF, editor. Encyclopedia of polymer science and technology. Hoboken, NJ: John Wiley & Sons; 2011.
53. Li F, Kang Z, Huang X, Wang X-G, Zhang G-J. Preparation of zirconium carbide foam by direct foaming method. J Eur Ceram Soc. 2014;34:3513–20.
54. Wang B, Matsumaru K, Yang J, Fu Z, Ishizaki K. Mechanical behavior of cellular borosilicate glass with pressurized Ar-filled closed pores. Acta Mater. 2012;60:4185–93.
55. Kim Y-W, Kim S-H, Xu X, Choi C-H, Park CB, Kim H-D. Fabrication of porous preceramic polymers using carbon dioxide. J Mater Sci Lett. 2002;21:1667–9.

56. Wolff F, Ceron Nicolat B, Fey T, Greil P, Münstedt H. Extrusion foaming of a preceramic silicone resin with a variety of profiles and morphologies. Adv Eng Mater. 2012;14:1110–5.
57. Ceron-Nicolat B, Wolff F, Dakkouri-Baldauf A, Fey T, Münstedt H, Greil P. Graded cellular ceramics from continuous foam extrusion. Adv Eng Mater. 2012;14:1097–103.
58. Wolff F, Münstedt H. Continuous direct melt foaming of a preceramic polymer using carbon dioxide: extrusion device and first results. J Mater Sci. 2011;46:6162–7.
59. Kim Y-W, Kim S-H, Wang C, Park CB. Fabrication of microcellular ceramics using gaseous carbon dioxide. J Am Ceram Soc. 2003;86:2231–3.
60. Kim Y-W, Park CB. Processing of microcellular preceramics using carbon dioxide. Compos Sci Technol. 2003;63:2371–7.
61. Østergaard MB, Petersen RR, König J, Bockowski M, Yue Y. Foam glass obtained through high-pressure sintering. J Am Ceram Soc. 2018;101:3917–23.
62. Akthar FK, Evans JRG. High porosity (>90%) cementitious foams. Cem Concr Res. 2010;40:352–8.
63. Bourret J, Michot A, Tessier-Doyen N, Naït-Ali B, Pennec F, Alzina A, et al. Thermal conductivity of very porous kaolin-based ceramics. J Am Ceram Soc. 2014;97:938–44.
64. Kearns M, Blenkinsop P. Manufacture of a novel porous metal. Met Mater. 1987;3:85–8.
65. Greiner C, Oppenheimer SM, Dunand DC. High strength, low stiffness, porous NiTi with superelastic properties. Acta Biomater. 2005;1:705–16.
66. Murray NGD, Dunand DC. Effect of thermal history on the superplastic expansion of argon-filled pores in titanium: Part I kinetics and microstructure. Acta Mater. 2004;52:2269–78.
67. Murray NGD, Dunand DC. Effect of thermal history on the superplastic expansion of argon-filled pores in titanium: Part II modeling of kinetics. Acta Mater. 2004;52:2279–91.
68. Baldwin DF, Park CB, Suh NP. A microcellular processing study of poly (ethylene terephthalate) in the amorphous and semicrystalline states. Part I: Microcell nucleation. Polym Eng Sci. 1996;36:1437–45.
69. Martini-Vvedensky JE, Suh NP, Waldman FA. Microcellular closed cell foams and their method of manufacture. U.S. Patent 4,473,665. 1984.
70. Arranz-Otaegui A, Carretero LG, Ramsey MN, Fuller DQ, Richter T. Archaeobotanical evidence reveals the origins of bread 14,400 years ago in northeastern Jordan. Proc Natl Acad Sci. 2018;115:7925–30.
71. Rathnayake H, Navaratne S, Navaratne C. Porous crumb structure of leavened baked products. Int. J Food Sci. 2018:2018:1–15.
72. Kishimoto A, Higashiwada T, Takahara M, Hayashi H. Solid state foaming and free-forming of closed pore utilizing the superplasticity of zirconia ceramics. Mater Sci Forum. 2007;544–545:641–4.
73. Kishimoto A, Hanao M, Hayashi H. Improvement in the specific strength by arranging closed pores in fully densified zirconia ceramics. Adv Eng Mater. 2009;11:96–100.
74. Wakiyama M, Waku K, Hayashi H, Kishimoto A. Fabrication of closed-pore inclusive low-permittivity substrates insensitive to ambient humidity. J Ceram Soc Jpn. 2009;117:1013–6.
75. Yamaoka H, Hayashi H, Kishimoto A. Applicability of nitride powders as foaming agents in superplastically foamed ceramics. J Ceram Soc Jpn. 2009;117:1233–5.
76. Wakiyama M, Hayashi H, Kishimoto A. Alumina based low permittivity substrate utilizing superplastically foaming method. J Ceram Soc Jpn. 2010;118:1090–3.
77. Kishimoto A, Nishino Y, Hayashi H. Patterning of closed pores utilizing the superplastically foaming method. In: Munir ZA, Ohji T, Hotta Y, editors. Innovative processing and manufacturing of advanced ceramics and composites. Hoboken, NJ: Wiley, 2011.
78. Kishimoto A. Superplastically foaming method for inclusion of closed pores in fully densified ceramics. J Ceram Soc Jpn. 2013;121:527–33.
79. Kishimoto A, Okada M, Teranishi T, Hayashi H. Maintaining the mechanical strength of La-, Y-co-substituted zirconia porous ceramics through the superplastically foaming method. Mater Sci Eng A. 2013;581:98–103.
80. Kishimoto A, Obata M, Waku K, Hayashi H. Mechanical and electrical properties of superplastically foamed titania-based ceramics. Ceram Int. 2009;35:1441–5.
81. Jiang C, Huang S, Li G, Zhang X, Cheng X. Formation of closed-pore foam ceramic from granite scraps. Ceram Int. 2018;44:3469–71.
82. Zheng Y, Li H, Zhou W, Zhang X, Ye G. Combustion synthesis and characteristics of aluminum oxynitride ceramic foams. Ceram Int. 2012;38:5139–44.
83. Narayanan N, Ramamurthy K. Structure and properties of aerated concrete: a review. Cem Concr Compos. 2000;22:321–9.
84. Hlaváček P, Šmilauer V, Škvára F, Kopecký L, Šulc R. Inorganic foams made from alkali-activated fly ash: mechanical, chemical and physical properties. J Eur Ceram Soc. 2015;35:703–9.
85. Kozlowski M. Lightweight plastic materials. In: El-Sonbati A, editor. Chapter 14 in thermoplastic elastomers. London: IntechOpen; 2012.
86. Chen X, Lu A, Qu G. Preparation and characterization of foam ceramics from red mud and fly ash using sodium silicate as foaming agent. Ceram Int. 2013;39:1923–9.
87. Zhou M, Ge X, Wang H, Chen L, Chen X. Effect of the CaO content and decomposition of calcium-containing minerals on properties and microstructure of ceramic foams from fly ash. Ceram Int. 2017;43:9451–7.
88. Lassinantti Gualtieri M, Colombini E, Mazzini D, Alboni C, Manfredini T, Siligardi C. The effect of alkaline earth carbonates on the microstructure and mechanical properties of impermeable and lightweight ceramics. J Eur Ceram Soc. 2018;38:5563–8.
89. Hashimoto S, Umeda T, Hirao K, Kondo N, Zhou Y, Hyuga H, et al. Fabrication and characterization of porous ZrO_2 with a high volume fraction of fine closed pores. J Eur Ceram Soc. 2013;33:61–6.
90. Hashimoto S, Umeda T, Hirao K, Kondo N, Hyuga H, Zhou Y, et al. Energy efficient synthesis of porous ZrO_2 with fine closed pores by microwave irradiation. Mater Lett. 2013;93:293–6.
91. Bai J, Yang X, Xu S, Jing W, Yang J. Preparation of foam glass from waste glass and fly ash. Mater Lett. 2014;136:52–4.
92. Fernandes HR, Tulyaganov DU, Ferreira JMF. Production and characterisation of glass ceramic foams from recycled raw materials. Adv Appl Ceram. 2009;108:9–13.
93. Tulyaganov DU, Fernandes HR, Agathopoulos S, Ferreira JMF. Preparation and characterization of high compressive strength foams from sheet glass. J Porous Mat. 2006;13:133–9.

94. Lv DS, Li XH, Wang L, Du JJ, Zhang J. Effect of carbon as foaming agent on pore structure of foam glass. Adv Mater Res. 2010;105–106:765–8.
95. Hesky D, Aneziris CG, Groß U, Horn A. Water and waterglass mixtures for foam glass production. Ceram Int. 2015;41:12604–13.
96. Qu Y-N, Xu J, Su Z-G, Ma N, Zhang X-Y, Xi X-Q, et al. Lightweight and high-strength glass foams prepared by a novel green spheres hollowing technique. Ceram Int. 2016;42:2370–7.
97. Qu Y-N, Su Z-G, Xu J, Huo W-L, Song K-C, Wang Y-L, et al. Preparation of ultralight glass foams via vacuum-assisted foaming. Mater Lett. 2016;166:35–8.
98. Wu JP, Boccaccini AR, Lee PD, Kershaw MJ, Rawlings RD. Glass ceramic foams from coal ash and waste glass: production and characterisation. Adv Appl Ceram. 2006;105:32–9.
99. Zhang Q, He F, Shu H, Qiao Y, Mei S, Jin M, et al. Preparation of high strength glass ceramic foams from waste cathode ray tube and germanium tailings. Constr Build Mater. 2016;111:105–10.
100. Guo HW, Gong YX, Gao SY. Preparation of high strength foam glass–ceramics from waste cathode ray tube. Mater Lett. 2010;64:997–9.
101. Li Z, Luo Z, Li X, Liu T, Guan L, Wu T, et al. Preparation and characterization of glass–ceramic foams with waste quartz sand and coal gangue in different proportions. J Porous Mater. 2016;23:231–8.
102. Zhu M, Ji R, Li Z, Wang H, Liu L, Zhang Z. Preparation of glass ceramic foams for thermal insulation applications from coal fly ash and waste glass. Constr Build Mater. 2016;112:398–405.
103. Li Z, Li X, Tang Y, Liu T, Wu T, Hao X, et al. Sintering behaviour and characterisation of low-cost ceramic foams from coal gangue and waste quartz sand. Adv Appl Ceram. 2016;115:377–83.
104. König J, Petersen RR, Yue Y. Influence of the glass–calcium carbonate mixture's characteristics on the foaming process and the properties of the foam glass. J Eur Ceram Soc. 2014;34:1591–8.
105. König J, Petersen RR, Iversen N, Yue Y. Suppressing the effect of cullet composition on the formation and properties of foamed glass. Ceram Int. 2018;44:11143–50.
106. Petersen RR, König J, Yue Y. The mechanism of foaming and thermal conductivity of glasses foamed with MnO_2. J Non Cryst Solids. 2015;425:74–82.
107. König J, Petersen RR, Yue Y. Influence of the glass particle size on the foaming process and physical characteristics of foam glasses. J Non Cryst Solids. 2016;447:190–7.
108. Østergaard MB, Petersen RR, König J, Yue Y. Effect of alkali phosphate content on foaming of CRT panel glass using Mn_3O_4 and carbon as foaming agents. J Non Cryst Solids. 2018;482:217–22.
109. König J, Petersen RR, Yue Y, Suvorov D. Gas-releasing reactions in foam-glass formation using carbon and MnxOy as the foaming agents. Ceram. Int. 2017;43:4638–46.
110. Lebullenger R, Chenu S, Rocherullé J, Merdrignac-Conanec O, Cheviré F, Tessier F, et al. Glass foams for environmental applications. J Non Cryst Solids. 2010;356:2562–8.
111. Li X, Zheng M, Li R, Yuan G, Zhou G, Zhu X, et al. Preparation, microstructure, properties and foaming mechanism of a foamed ceramics with high closed porosity. Ceram Int. 2019;45:11982–8.
112. da Silva RC, Kubaski ET, Tenório-Neto ET, Lima-Tenório MK, Tebcherani SM. Foam glass using sodium hydroxide as foaming agent: study on the reaction mechanism in soda-lime glass matrix. J Non Cryst Solids. 2019;511:177–82.
113. Chen B, Luo Z, Lu A. Preparation of sintered foam glass with high fly ash content. Mater Lett. 2011;65:3555–8.
114. Taurino R, Lancellotti I, Barbieri L, Leonelli C. Glass–ceramic foams from borosilicate glass waste. Int J Appl Glass Sci. 2014;5:136–45.
115. Kaz'mina OV, Vereshchagin VI, Semukhin BS. Structure and strength of foam-glass-crystalline materials produced from a glass granulate. Glass Phys Chem. 2011;37:371.
116. Scarinci G, Brusatin G, Bernardo E. Glass foams. In: Brusatin G, Colombo P, editors. Chapter 2.7 in Cellular ceramics: structure, manufacturing, properties and applications. Chichester: Wiley; 2005.
117. Defrancesco F, Tomasi A, Soraru GD. Expanded materials from quartz-porphyrite sands. J Mater Sci. 1987;22:2493–6.
118. Rahaman MN. Ceramic processing and sintering. Boca Raton, FL: CRC Press, 2003.
119. Villegas M, Sierra T, Lucas F, Fernández JF, Caballero AC. Oxidation treatments for SiC particles and its compatibility with glass. J Eur Ceram Soc. 2007;27:861–5.
120. Liu T, Li X, Guan L, Liu P, Wu T, Li Z, et al. Low-cost and environment-friendly ceramic foams made from lead–zinc mine tailings and red mud: foaming mechanism, physical, mechanical and chemical properties. Ceram Int. 2016;42:1733–9.
121. Cao F, Ding Y, Chen L, Chen C, Fang Z. Fabrication and characterization of boron nitride bulk foam from borazine. Mater Design. 2014;54:610–5.
122. Liu T, Lin C, Liu J, Han L, Gui H, Li C, et al. Phase evolution, pore morphology and microstructure of glass ceramic foams derived from tailings wastes. Ceram Int. 2018;44:14393–400.
123. Liu T, Tang Y, Li Z, Wu T, Lu A. Red mud and fly ash incorporation for lightweight foamed ceramics using lead-zinc mine tailings as foaming agent. Mater Lett. 2016;183:362–4.
124. Liu T, Tang Y, Han L, Song J, Luo Z, Lu A. Recycling of harmful waste lead-zinc mine tailings and fly ash for preparation of inorganic porous ceramics. Ceram Int. 2017;43:4910–8.
125. Marangoni M, Secco M, Parisatto M, Artioli G, Bernardo E, Colombo P, et al. Cellular glass–ceramics from a self foaming mixture of glass and basalt scoria. J Non Cryst Solids. 2014;403:38–46.
126. Lima ECD, Sartoratto PPC, Ayres AM, Oliveira SB. Aluminum/sodium pliveirahosphate-based closed cell ceramic foams. J Non Cryst Solids. 2001;279:60–71.
127. Grader GS, Shter GE, Hazan YD. Novel ceramic foams from crystals of $AlCl_3(Pri_2O)$ complex. J Mater Res. 2011;14:1485–94.
128. Boccaccini AR, Veronesi P, Leonelli C. Microwave processing of glass matrix composites containing controlled isolated porosity. J Eur Ceram Soc. 2001;21:1073–80.
129. Kim E, Kim K, Lee H, Kim I, Song O. Effects of molding pressure and sintering temperature on properties of foamed glass without blowing agent. J Korean Ceram Soc. 2019;56:178–83.
130. Li NA, Zhang X-Y, Qu Y-N, Xu J, Ma N, Gan KE, et al. A simple and efficient way to prepare porous mullite matrix ceramics via directly sintering SiO_2-Al_2O_3 microspheres. J Eur Ceram Soc. 2016;36:2807–12.
131. Luo Y, Zheng S, Ma S, Liu C, Wang X. Preparation of sintered foamed ceramics derived entirely from coal fly ash. Constr Build Mater. 2018;163:529–38.
132. Zhang X-Y, Lan T, Li NA, Wu J-M, Huo W-L, Ma N, et al. Porous silica ceramics with uniform pores from the in-situ foaming process of silica poly-hollow microspheres in inert atmosphere. Mater Lett. 2016;182:143–6.

133. Xu C, Wang S, Flodström K, Mao X, Guo J. Cellular silica-based ceramics prepared by direct foaming at high temperature. Ceram Int. 2010;36:923–7.
134. Sjöblom J, Stenius P, Simon S, Grimes BA. Emulsion stabilization. In: Tadros T, editor. Encyclopedia of colloid and interface science. Berlin, Heidelberg: Springer, 2013; p. 415–54.
135. García-Tuñón E, Machado GC, Schneider M, Barg S, Bell RV, Saiz E. Complex ceramic architectures by directed assembly of 'responsive' particles. J Eur Ceram Soc. 2017;37:199–211.
136. Huo W, Zhang X, Chen Y, Hu Z, Wang D, Yang J. Ultralight and high-strength bulk alumina/zirconia composite ceramic foams through direct foaming method. Ceram Int. 2019;45:1464–7.
137. Arditty S, Schmitt V, Giermanska-Kahn J, Leal-Calderon F. Materials based on solid-stabilized emulsions. J Colloid Interface Sci. 2004;275:659–64.
138. Menner A, Verdejo R, Shaffer M, Bismarck A. Particle-stabilized surfactant-free medium internal phase emulsions as templates for porous nanocomposite materials: poly-pickering-foams. Langmuir. 2007;23:2398–403.
139. Ramanath G, D'Arcy-Gall J, Maddanimath T, Ellis AV, Ganesan PG, Goswami R, et al. Templateless room-temperature assembly of nanowire networks from nanoparticles. Langmuir. 2004;20:5583–7.
140. Gonzenbach UT, Studart AR, Tervoort E, Gauckler LJ. Ultrastable particle-stabilized foams. Angew Chem Int Ed Engl. 2006;45:3526–30.
141. Gonzenbach UT, Studart AR, Steinlin D, Tervoort E, Gauckler LJ. Processing of particle-stabilized wet foams into porous ceramics. J Am Ceram Soc. 2007;90:3407–14.
142. Wang M, Du H, Guo A, Hao R, Hou Z. Microstructure control in ceramic foams via mixed cationic/anionic surfactant. Mater Lett. 2012;88:97–100.
143. Chuanuwatanakul C, Tallon C, Dunstan DE, Franks GV. Controlling the microstructure of ceramic particle stabilized foams: influence of contact angle and particle aggregation. Soft Matter. 2011;7:11464–74.
144. Yu J, Yang J, Li H, Xi X, Huang Y. Study on particle-stabilized Si_3N_4 ceramic foams. Mater Lett. 2011;65:1801–4.
145. Sciamanna V, Nait-Ali B, Gonon M. Mechanical properties and thermal conductivity of porous alumina ceramics obtained from particle stabilized foams. Ceram Int. 2015;41:2599–606.
146. Bourret J, Tessier-Doyen N, Naït-Ali B, Pennec F, Alzina A, Peyratout CS, et al. Effect of the pore volume fraction on the thermal conductivity and mechanical properties of kaolin-based foams. J Eur Ceram Soc. 2013;33:1487–95.
147. Ahmad R, Ha J-H, Song I-H. Particle-stabilized ultra-low density zirconia toughened alumina foams. J Eur Ceram Soc. 2013;33:2559–64.
148. Yu J, Yang J, Li H, Huang Y. Pore structure control of Si3N4 ceramics based on particle-stabilized foams. J Porous Mat. 2012;19:883–8.
149. Pokhrel A, Park JG, Kim IJ. Wet foams hydrophobized by amphiphiles to give Al_2O_3 porous ceramics. AIP Conf Proc. 2012;1453:225–30.
150. Huo W-L, Zhang X-Y, Chen Y-G, Lu Y-J, Liu W-T, Xi X-Q, et al. Highly porous zirconia ceramic foams with low thermal conductivity from particle-stabilized foams. J Am Ceram Soc. 2016;99:3512–5.
151. Huo W, Chen Y, Zhang Z, Liu J, Yan S, Wu J-M, et al. Highly porous barium strontium titanate (BST) ceramic foams with low dielectric constant from particle-stabilized foams. J Am Ceram Soc. 2018;101:1737–46.
152. Chen Z, Li Z, Li J, Liu C, Lao C, Fu Y, et al. 3D printing of ceramics: a review. J Eur Ceram Soc. 2019;39:661–87.
153. Zocca A, Colombo P, Gomes CM, Günster J. Additive manufacturing of ceramics: issues, potentialities, and opportunities. J Am Ceram Soc. 2015;98:1983–2001.
154. Pokhrel A, Park J-G, Nam J-S, Cheong D-S, Kim I-J. Stabilization of wet foams for porous ceramics using amphiphilic particles. J Korean Ceram Soc. 2011;48:460–3.
155. Huo W-L, Qi F, Zhang X-Y, Ma N, Gan KE, Qu Y-N, et al. Ultralight alumina ceramic foams with single-grain wall using sodium dodecyl sulfate as long-chain surfactant. J Eur Ceram Soc. 2016;36:4163–70.
156. Ren J, Ying W, Zhao J, Xie J, Zhou G, Shi Y, et al. High-strength porous mullite ceramics fabricated from particle-stabilized foams via oppositely charged dispersants and surfactants. Ceram Int. 2019;45:6385–91.
157. Nielsen LF. Strength and stiffness of porous materials. J. Am. Ceram. Soc. 1990;73:2684–9.
158. Green DJ. Fracture toughness/young's modulus correlation for low-density fibrous silica bodies. J. Am. Ceram. Soc. 1983;66:288–92.
159. Green DJ. Mechanical behavior of lightweight ceramics. Fracture mechanics of ceramics. Berlin: Springer, 1986; p. 39–59.
160. Haggerty JS, Lighfoot A, Ritter JE, Nair SV. High strength, porous, brittle materials. MRS Online Proce Libr Arch. 1990;207:71–76.
161. Gibson LJ, Ashby MF. Cellular solids: structure and properties. Cambridge: Cambridge University Press, 1999.
162. Colombo P, Bernardo E. Cellular structures. In: Riedel R, Chen I, editors. Ceramics science and technology. Weinheim: Wiley-VCH, 2014.
163. Salvini VR, Pandolfelli VC, Spinelli D. Mechanical properties of porous ceramics. In: Al-Naib UMB, editor. Chapter 10 in Recent Advances in Porous Ceramics. London: IntechOpen; 2018.
164. Ashby M. The properties of foams and lattices. Philos Trans Royal Soc A. 2005;364:15–30.
165. Deshpande V, Ashby M, Fleck N. Foam topology: bending versus stretching dominated architectures. Acta Mater. 2001;49:1035–40.
166. Sanders WS, Gibson L. Mechanics of hollow sphere foams. Mater Sci Eng A. 2003;347:70–85.
167. Brezny R, Green DJ. Mechanical behavior of cellular ceramics. In: Cahn RW, Haasen P, Kramer EJ, editors. Materials science and technology. Weinheim: Wiley-VCH, 2006.
168. Dittmann J, Willenbacher N. Micro structural investigations and mechanical properties of macro porous ceramic materials from capillary suspensions. J Am Ceram Soc. 2014;97:3787–92.
169. Colombo P, Bernardo E, Biasetto L. Novel microcellular ceramics from a silicone resin. J Am Ceram Soc. 2004;87:152–4.
170. Brezny R, Green DJ. The effect of cell size on the mechanical behavior of cellular materials. Acta Metall Mater. 1990;38:2517–26.
171. Brezny R, Green D. Characterization of edge effects in cellular materials. J Mater Sci. 1990;25:4571–8.
172. Maxwell JCL. On the calculation of the equilibrium and stiffness of frames. Lond Edinb Dubl Phil Mag J Sci. 1864;27:294–9.
173. He Z, Wang F, Zhu Y, Wu H, Park HS. Mechanical properties of copper octet-truss nanolattices. J Mech Phys Solids. 2017;101:133–49.
174. Kaur M, Han SM, Kim WS. Three-dimensionally printed cellular architecture materials: perspectives on fabrication, material advances, and applications. MRS Commun. 2016;7:8–19.

175. Fleck NA, Ashby MF, Deshpande VS. The topology of cellular structures. In: Drew HR, Pellegrino S, editors. New approaches to structural mechanics, shells and biological structures. Dordrecht: Springer Science & Business Media, 2013.
176. Bauer J, Hengsbach S, Tesari I, Schwaiger R, Kraft O. High-strength cellular ceramic composites with 3D microarchitecture. Proc Natl Acad Sci. 2014;111:2453–8.
177. Muth JT, Dixon PG, Woish L, Gibson LJ, Lewis JA. Architected cellular ceramics with tailored stiffness via direct foam writing. Proc Natl Acad Sci. 2017;114:1832–7.
178. Minas C, Carnelli D, Tervoort E, Studart AR. 3D Printing of emulsions and foams into hierarchical porous ceramics. Adv Mater. 2016;28:9993–9.
179. Chen A-N, Li M, Wu J-M, Cheng L-J, Liu R-Z, Shi Y-S, et al. Enhancement mechanism of mechanical performance of highly porous mullite ceramics with bimodal pore structures prepared by selective laser sintering. J Alloys Compd. 2019;776:486–94.
180. Prabhu S, Raja V, Nikhil R. Applications of cellular materials-an overview. Appl Mech Mater. 2015;766:511–7.
181. Jung J-Y, Pissarenko A, Yaraghi NA, Naleway SE, Kisailus D, Meyers MA, et al. A comparative analysis of the avian skull: Woodpeckers and chickens. J Mech Behav Biomed. 2018;84:273–80.
182. Mayeaux BM, Collins TE, Jerman GA, McDanels SJ, Piascik RS, Russell RW, et al. Materials analysis: a key to unlocking the mystery of the Columbia tragedy. JoM. 2004;56:20–30.
183. Aegerter MA, Leventis N, Koebel MM. Aerogels handbook. New York, NY: Springer Science & Business Media; 2011.
184. Alvarez-Lainez M, Rodriguez-Perez M, De Saja J. Thermal conductivity of open-cell polyolefin foams. J Polym Sci B Polym Phys. 2008;46:212–21.
185. Kittel C, McEuen P, McEuen P. Introduction to solid state physics. New York, NY: Wiley; 1976.
186. Gusev YV. The quasi-low temperature behaviour of specific heat. R Soc Open Sci. 2019;6:171285.
187. Schuetz MA, Glicksman LR. A basic study of heat transfer through foam insulation. J Cell Plast. 1984;20:114–21.
188. Klemens PG. Theory of the thermal conductivity of amorphous solids. In: Ashworth T, Smith DR, editors. Thermal conductivity, vol. 18. Boston, MA: Springer, 1985; p. 307–314.
189. Rambo C, Cao J, Rusina O, Sieber H. Manufacturing of biomorphic (Si, Ti, Zr)-carbide ceramics by sol–gel processing. Carbon. 2005;43:1174–83.
190. Yaws CL. Transport properties of chemicals and hydrocarbons. Norwich, NY: William Andrew; 2009.
191. Vedula VR, Green DJ, Hellmann JR. Thermal fatigue resistance of open cell ceramic foams. J Eur Ceram Soc. 1998;18:2073–80.
192. Nakayama J. Thermal shock resistance of ceramic materials. Fracture Mechanics of ceramics. Berlin: Springer, 1974; p. 759–78.
193. Music D, Stelzer B. Intrinsic thermal shock behavior of common rutile oxides. Physics. 2019;1:290–300.
194. Lu TJ, Fleck NA. The thermal shock resistance of solids. Acta Mater. 1998;46:4755–68.
195. Boccaccini AR, Ondracek G. The quantitative microstructure-property correlations of composite and porous materials: an engineering tool for designing new materials. In: Pyrz R, editor. IUTAM symposium on microstructure-property interactions in composite materials. Dordrecht: Springer; 1995; p. 27–38.
196. Arnold M, Boccaccini A, Ondracek G. Theoretical and experimental considerations on the thermal shock resistance of sintered glasses and ceramics using modelled microstructure-property correlations. J. Mater. Sci. 1996;31:463–9.
197. Jin Y, Chou Y. Thermal and mechanical properties of porous Y-PSZ/zircon composites. Mater Res Innov. 1998;1:227–30.
198. Bunn P, Mottram J. Manufacture and compression properties of syntactic foams. Composites. 1993;24:565–71.
199. Bardella L, Genna F. On the elastic behavior of syntactic foams. Int J Solids Struct. 2001;38:7235–60.
200. Wu G, Dou Z, Sun D, Jiang L, Ding B, He B. Compression behaviors of cenosphere–pure aluminum syntactic foams. Scr Mater. 2007;56:221–4.
201. Heat-insulating materials and sound-absorbing materials. In: Zhang H, editor. Building materials in civil engineering. Sawston: Woodhead Publishing; 2011; p. 304–423.
202. Krämer C, Schauerte M, Kowald TL, Trettin RHF. Three-phase-foams for foam concrete application. Mater. Charact. 2015;102:173–9.
203. Alexanderson J. Relations between structure and mechanical properties of autoclaved aerated concrete. Cem Concr Res. 1979;9:507–14.
204. Kudyakov AI, Kopanitsa NO, Sarkisov JS, Kasatkina AV, Prischepa IA. Foam concrete of increased strength with the thermomodified peat additives. IOP Conf Ser: Mater Sci Eng. 2015;71:012012.
205. Liu Z, Zhao K, Hu C, Tang Y. Effect of water-cement ratio on pore structure and strength of foam concrete. Adv Mater Sci Eng. 2016;2016:9.
206. Yu XG, Luo SS, Gao YN, et al. Pore structure and microstructure of foam concrete. Adv Mater Res. 2011;177:530–2.
207. Mydin MAO, Wang YC. Mechanical properties of foamed concrete exposed to high temperatures. Constr Build Mater. 2012;26:638–54.
208. Ozcivici E, Singh RP. Syntactic closed-cell foams based on silicon carbide. MRS Proc. 2004;851:NN11.7.1-6.
209. Ozcivici E, Singh RP. Fabrication and characterization of ceramic foams based on silicon carbide matrix and hollow alumino-silicate spheres. J Am Ceram Soc. 2005;88:3338–45.
210. Sharafat S, Aoyama A, Morley N, Ghoniem N, Williams B, Seline J. Development of closed-cell syntactic SiC-foam for flow channel inserts. In: 23rd IEEE/NPSS Symposium on Fusion Engineering, 2009; p. 1–4.
211. Vakifahmetoglu C, Buldu M, Karakuscu A, Ponzoni A, Assefa D, Soraru GD. High surface area carbonous components from emulsion derived SiOC and their gas sensing behavior. J Eur Ceram Soc. 2015;35:4447–52.
212. Ma S, Chen W, Zhao W. Mechanical properties and associated seismic isolation effects of foamed concrete layer in rock tunnel. J Rock Mech Rock Eng. 2019;11:159–71.
213. Movahedi N, Murch GE, Belova IV, Fiedler T. Functionally graded metal syntactic foam: fabrication and mechanical properties. Mater Design. 2019;168:107652.
214. Yamamoto JK, Kata K, Shimada Y. Fabrication of controlled porosity in a tape cast glass ceramic substrate material. Mater Lett. 1989;8:278–82.
215. Lichtenecker K. Die dielektrizitatskonstante naturlicher und kunstlicher mischkorper. Phys Z. 1926;27:115–58.
216. Yamamoto JK, Lanagan MT, Bhalla AS, Newnham RE, Cross LE. Dielectric properties of microporous glass in the microwave region. J Am Ceram Soc. 1989;72:916–21.

217. Ciomaga CE, Padurariu L, Curecheriu LP, et al. Using multi-walled carbon nanotubes in spark plasma sintered Pb ($Zr_{0.47}Ti_{0.53}$) O_3 ceramics for tailoring dielectric and tunability properties. J Appl Phys. 2014;116:164110.
218. Barta J, Manela M, Fischer R. Si_3N_4 and Si_2N_2O for high performance radomes. Mater Sci Eng. 1985;71:265–72.
219. Zhou L, Pei Y, Zhang R, Fang D. Design for broadband high-temperature radome wall with graded porous structure. AIAA J. 2012;50:1956–63.
220. Lu TJ, Hess A, Ashby M. Sound absorption in metallic foams. J. Appl. Phys. 1999;85:7528–39.
221. Liu P, Chen G-F. Porous materials: processing and applications. Oxford: Butterworth-Heinemann, 2014.
222. Frank G, Christian E, Dietmar K. A novel production method for porous sound-absorbing ceramic material for high-temperature applications. Int J Appl Ceram Technol. 2011;8:646–52.
223. Carlesso M, Molotnikov A, Krause T, Tushtev K, Kroll S, Rezwan K, et al. Enhancement of sound absorption properties using topologically interlocked elements. Scripta Mater. 2012;66:483–6.
224. Carlesso MV. Functional porous ceramic materials with sound absorption properties for high temperature applications. PhD thesis, 2014.
225. Maier HR. Porous ceramics functional cavities for system innovation. In: Heinrich JG, Aldinger F, editors. Ceramic materials and components for engines. Weinheim: Wiley-VCH; 2001; p. 537–542.
226. Byakova A, Gnyloskurenko S, Bezimyanniy Y, Nakamura T. Closed-cell aluminum foam of improved sound absorption ability: Manufacture and properties. Metals. 2014;4:445–54.

AUTHOR BIOGRAPHIES

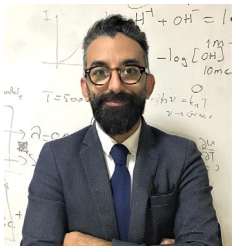

Cekdar Vakifahmetoglu (Vakif Ahmetoglu) is professor of Materials Science and Engineering at the Izmir Institute of Technology, Turkey. After obtaining his BS (2002) and MSc (2005) degrees from the Middle East Technical University (METU, Ankara, Turkey) department of Metallurgical and Materials Engineering, he completed his PhD on porous polymer-derived ceramics (PDCs) under the supervision of Prof. Ing. Paolo Colombo (University of Padova, Italy, 2010). Following that he joined the group of Prof. Dr. Richard E. Riman (Rutgers, The State University of New Jersey, Department of Materials Science and Engineering, USA) as a postdoc where he started to be involved in hydro&solvothermal methods for solution crystallization and densification of inorganic solids at low temperatures. He was a Marie-Curie fellow, and recently awarded by the Alexander von Humboldt (AvH) foundation (2019) for research at the Technical University of Berlin (Germany) with Prof. Dr Aleksander Gurlo. His current research is devoted mainly to the processing of porous components ranging from particulates to foams, waste recycling & green manufacturing methods, and low temperature densification techniques for glass and ceramic artifacts.

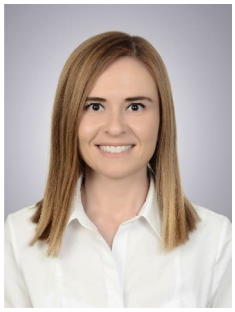

Tugce Semerci is a PhD candidate and research assistant in the Department of Materials Science and Engineering, Izmir Institute of Technology (IZTECH, Izmir, Turkey) under the supervision of Prof. Dr Cekdar Vakif Ahmetoglu. She received her BS degree (2012) in Physics, and MSc degree (2015) in Materials Science and Engineering both from IZTECH. She studied superconducting single crystals for Terahertz bolometric detectors during her MSc studies. Her current research interests are in the formation of highly porous ceramic components especially those derived from preceramic polymers, and their high temperature applications.

Gian Domenico Soraru is professor of Materials Science and Technology at the University of Trento, Italy. After graduation from the University of Padova, in between 1987-1989 he joined the group of Prof. J. D. Mackenzie at UCLA as postdoc where he started to be involved in the PDCs field studying silicon oxycarbide glasses from gel-derived precursors. His current research interests are in the synthesis and characterization of porous PDC including aerogels foams and felts for energy and environmental application.

How to cite this article: Vakifahmetoglu C, Semerci T, Soraru GD. Closed porosity ceramics and glasses. *J Am Ceram Soc*. 2020;103:2941–2969. https://doi.org/10.1111/jace.16934